Elaborato di Tesi ...

Titolo progetto di tesi ...

Progetto svolto da:
Andrea Bortolossi
Matr. 783023

Anno Accademico 2013–2014

Indice

Capitolo 1

Introduction

1.1 Brief history of VLSI devices

In 1947 John Bardeen, William Shockley and Walter Brattain (three scientists of Bell Telephone Labs) invented the bipolar transistor and since that crucial point there has been a growth of the semiconductor industry never known before, with serious impact on the way people work and live today.

Before reach the functionality and the miniaturization of modern devices, some fundamental steps has been made. In 1958 the first intagrated circuits (IC) was produced, followed by the introduction of the first MOSFET(1960) and CMOS(1963). Into these inventions the first microprocessor(1971) sank his roots and since that time until present, an ever-increasing progress has continued, according to the indication of *Moore's Law* (formulated by Gordton Moore in 1965).

These events led microelectronic industry at the doors of the VLSI era (Very-Large-Scale-Integration). Indeed in the last thirty years the benefits of miniaturization have been the key in the evolutionary progress leading to today's computers, wireless units, and comunication systems that offer superior performance, dramatically reduced cost per function, and much reduced physical size.

The large worldwide investment in VLSI technology constitutes a formidable driving force that guarantee the continued progress in IC integration density and speed, for as long as physical principles will allow.

From this point we want start and remark that the aim of numerical simulations is the comprehension of the physical phenomenon which lies behind the function of modern device.

Even if many commercial software are able to resolve different physic situations, they are often specialized on precise physic branch: obviously this

strategic choice guarantees more efficiency but it implies a lost in generality. The conseguence is that the work of the model analyst became harder when he have to afford problems located in the middle of different phenomenon.

Consider, as example, the functionality of a new device, which its electric behaviour is strong influeced by its mechanical response. Basically you are interested to the resolution of Maxwell's law (which is well performed by SDE-VICE simulator) and the Navier-Lamè equations (which is well performed by COMSOL simulator). Now the question is: how to put in comunication the different outputs? Take into account that it's not possbile known precisely how the above programs resolves the equations, which implies a relevant risk when you decide to combine the solutions. In other words the development of an own code is at least desirable and possibly helpful: the main advantage is the total control on simulation procedure and the possibility of fully customize, the major drawback is that the improvement of a personal code needs time and human resources, which in many cases are not avaible.

The FEMOS project (*Finite Element Method Oriented Solver*) tries to overcome the above limitations. Even if modern devices present innovative and unexpected behaviour, we can't avoid the treatment of the classical semiconductor devices from the simulation possibilties of FEMOS. This thesis found its origin in the development of this achievement, but as subject covered a spread wide area in terms of models and kind of devices and we focus on:

- development of a finite element based simulator for semiconductor devices which deals with multiple generation/recombination and mobility models;

- check solutions obtained against commercial software (SDEVICE);

- definition and implementation of a new way to compute the current density inside the device;

- extension of the residual method presented in referenza for the 3D case;

- evaluation of the possibility to extend the residual method at the computation of the current density inside the device.

Capitolo 2

Semiconductor model

In this chapter we shall present the basic physics properties of semiconductor material accordingly with the quantum mechanics theory [YT09]. The Drift-Diffusion model is then presented.

2.1 Basic Device Physics

This section covers the basic concepts of semiconductor device physics. As the most used material in the fabrication of VLSI devices is silicon, in the follow we will focus on it.

2.1.1 Intrinsic semiconductor

In a silicon crystal each atom has four valence electrons to share with its four nearest neighboring atoms. The valence electrons are shared in a paired configuration called a covalent bond. The most important result of the application of quantum mechanics to the description of electrons in a solid is that the allowed energy levels of electrons are grouped into bands. The bands are separated by regions of energy that the electrons in the solid cannot possess: forbidden gaps. The highest energy band that is completely filled by electron at 0[K] is called the *valence band* (E_V). The next higher energy band, separated by a frobidden gap from the valence band, is called the *conduction band* (E_C).

Because in silicon the band gap is on the order of 1 [eV], at room temperature a small fraction of the electrons are excited into the conduction band, leaving behind vacancies (called *holes*) in the valence band. In contrast, an insulator has a much larger forbidden gap making room-temperature conduction virtually impossible, while metals have partially filled conduction bands
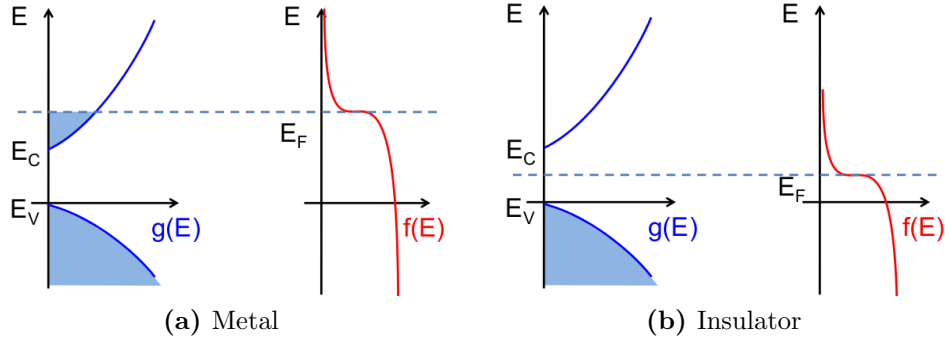
(a) Metal   **(b)** Insulator

Figura 2.1: Two typical examples of state density occupation (g(E)) and probability distribution (f(E)).

even at absolute zero temperature, this make them good conductors at any temperature.

A suitable formulation of che carrier concentration which is given, for electrons, by the follow integral:

$$n = \int_{E_c}^{\infty} g(E)f(E)\,dE \tag{2.1}$$

With $g(E)dE$ we indicate the number of electronic states per unit volume with an energy between E and $E + dE$ in the conduction band and $f(E)$ is a suitable probability ditribution.

The energy distribution of electrons in a solid is governed by the laws of Fermi-Dirac statistics. For a system in thermal equilibrium, the principal result of these statistics is the *Fermi-Dirac distribution function*, which gives the probability that an electronic state at energy E is occupied by an electron,

$$f_D(E) = \frac{1}{1 + exp\left(\dfrac{E - E_f}{k_B T}\right)} \tag{2.2}$$

here $k_B = 1.38 \times 10^{-23}[J/K]$ is Boltzmann's constant, T is the absolute temperature and E_f is the *Fermi level*.

Definition 2.1. The Fermi level (E_f) is the energy at which the probability of occupation of an energy state by an electron is exactly one-half.

In most cases when the energy is at least several $k_B T$ above or below the Fermi level (2.2) can be approximated with the Maxwell-Boltzmann statistics for classical particles, which read as follows:

$$f_D(E) \simeq f_{MB}(E) = \begin{cases} exp\left(-\dfrac{E - E_f}{KT}\right) & E \gg E_f \\ 1 - exp\left(-\dfrac{E_f - E}{KT}\right) & E \ll E_f \end{cases} \tag{2.3}$$

Fermi level plays an essential role in characterizing the equilibrium state of a stystem, it is important to keep in mind the sequent observation.

Observation 2.1. When two systems are in thermal equilibrium with no current flow between them, their Fermi levels must be equal, in other words for a continuous region of metals and/or semiconductors in contact, the Fermi level at thermal equilibrium is flat (spatially constant throughout the region).

In general (2.1) is a Fermi integral of the order 1/2 and must be evaluated numerically. In the case of non-degenerate semiconductor, Fermi levels stay at least $3KT/q$ below the edge of the conduction band (for holes we consider the same approximation above the valence band). The Fermi-Dirac distribution can be approximated by the Maxwell-Boltzmann distribution and (2.1) can be solved in the analytically way, obtaining,

$$n = N_c exp\left(-\frac{E_c - E_f}{KT}\right) \tag{2.4}$$

$$p = N_v exp\left(-\frac{E_f - E_v}{KT}\right) \tag{2.5}$$

where N_c and N_v are the *effective density of states*. In intrisic semiconductor $n = p$ and the *intrinsic Fermi level* E_i can be calculated using equations (2.4) and (2.5) as:

$$E_i = E_f = \frac{E_c + E_v}{2} - \frac{KT}{2} ln\left(\frac{N_c}{N_v}\right) \tag{2.6}$$

By replacing (2.6) in (2.4) we have the expression of the intrinsic carrier concentration $n_i = n = p$:

$$n_i = \sqrt{N_c N_v} exp\left(-\frac{E_g}{2KT}\right) \tag{2.7}$$

Observation 2.2. Since the thermal energy, $k_B T$ is muc smaller than the usual semiconductor bandgap E_g, the intrinsic Fermi level is very close to the midpoint between the conduction band and the valence band.

Equations (2.4) and (2.5) can be rewritten in terms of the intrinsic carrier density (n_i) and energy (E_i) :

$$n = n_i exp\left(\frac{E_f - E_i}{KT}\right) \tag{2.8}$$

$$p = n_i exp\left(\frac{E_i - E_f}{KT}\right) \tag{2.9}$$

Finally we remark a fundamental and useful relation holds at the thermical equilibrium

$$np = n_i^2 \tag{2.10}$$

this relation is usually note as *mass action law*.

One of the most used graphical tool for the anlysis of the functionality of devices is the band diagram Fig.2.2, which summarizes the informations presented above.
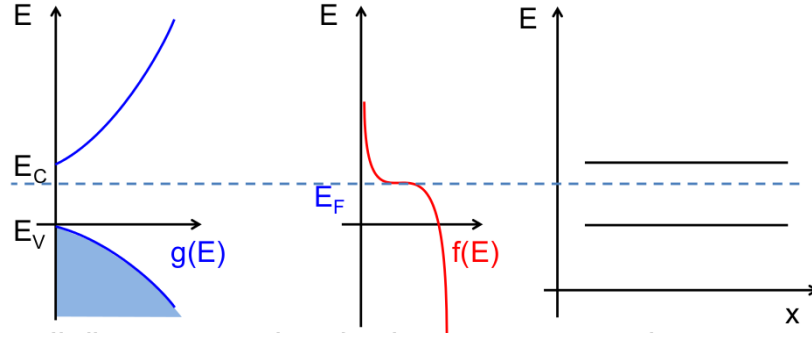
Figura 2.2: Construction of tha band diagram.

2.1.2   Extrinsic semiconductor

At room temperature intrinsic semiconductor has an extremely low free-carrier concentration, therefore, its resistivity is very high. In order to make semiconductor a better conductor it's usual add impurities atoms which introduce additional energy levels in the forbidden gap: these impurities are easily ionized adding either electrons to the conduction band or holes to the valence band. Here the electrical conductivity is dominated by the type and concentration of the impurity atoms.

In the case of silicon two are the types of impurities which are electrically active: those from column V such as arsenic or phosphorus, and those from column III such as boron or indium.

A column-V atom in a silicon lattice tends to have one extra electron loosely bonded after forming covalent bonds with other silicon atoms. In most cases, the thermal energy at room temperature is sufficient to ionize the impurity atom and free the extra electron to the conduction band. Such type of impurities are called *donors*; they become positively charged when ionized. Silicon material doped with column-V impurities or donors is called *n-type* silicon.

A column-III impurity atom in a silicon lattice tends to be deficient by one electron when forming covalent bonds with other silicon atoms. Such an impurity atom can also be ionized by accepting an electron from the valence band, which leaves a free-moving hole that contributes to electrical conduction. These impurities are called *acceptors*: they become negatively charged when ionized. Silicon material doped with column-III impurities or acceptors is called *p-type* silicon.

A p-type or an n-type is named as *extrinsic* silicon. In terms of the energy-band diagrams, donors add allowed electron states in the bandgap close to the conduction-band edge, while acceptors add allowed states just above the valence-band edge.

In contrast to intrinsic silicon, the Fermi level in an extrinsic silicon is not located at the midgap. The Fermi level in n-type silicon moves up towards the conduction band while in p-type silicon moves down towards the valence band. The exact position of the Fermi level depends on both the ionization energy and the concentration of dopants. For example, for an n-type material with a donor impurity concentration, N_d, the charge neutrality condition requires that

$$n = N_d^+ + p \tag{2.11}$$

where N_d^+ is the density of ionized donors. Similarly for a p-type material with acceptor impurity concentration N_a we have

$$p = N_a^- + n \tag{2.12}$$

For the sake of simplicity we consider in this work that at room temperature all impurties are ionized ($N_d = N_d^+$ and $N_a = N_a^-$). Typcally the magnitude of impurities is between $10^{16} * 10^{20} [cm^{-3}]$, while the usual intrinsic carrier concentration is almost $10^{10} [cm_3]$, for this reason we can approximate the equilibrium densities concentration:

$$n \simeq N_d \quad p \simeq \frac{n_i^2}{N_d}$$

$$\tag{2.13}$$

$$p \simeq N_a \quad n \simeq \frac{n_i^2}{N_a}$$

Take into account this approximation and substituting (2.4) and (2.5) in (2.11) and (2.12), solving the algebraic equationwe have

$$E_c - E_f = KTln\left(\frac{N_c}{N_d}\right) \tag{2.14}$$

$$E_f - E_v = KTln\left(\frac{N_v}{N_a}\right) \tag{2.15}$$

Equation (2.10) is indipendent of the dopant type and Fermi level position. Instead of using N_c, N_v and referring to E_c and E_v equation (2.14) and (2.15) can be written in a more useful form in terms of n_i and E_i defined by equations (2.7) and (2.6):

$$E_f - E_i = KTln\left(\frac{N_d}{n_i}\right) \tag{2.16}$$

$$E_i - E_f = KTln\left(\frac{N_a}{n_i}\right) \tag{2.17}$$

Observation 2.3. The distance between the Fermi level and the intrinsic Fermi level near the midgap is a logarithmic function of doping concentration.

As a consequences:

- non linearity relations between potential and desities,

- exponential dependence of densities from potential.

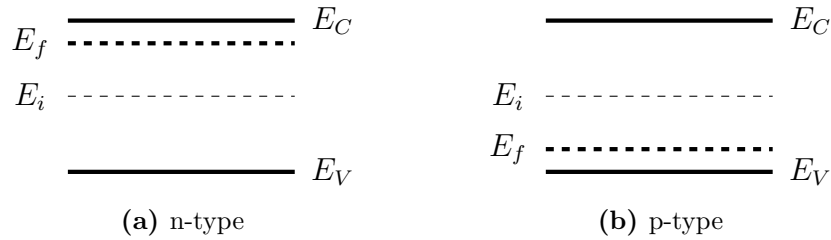**(a)** n-type   **(b)** p-type

Figura 2.3: Band diagrams of estrinsic silicon.

2.1.3   Densities at nonequilibrium condition

In VLSI device operation a nonequilibrium sistuations is often possible: the densities of one or both types of carriers depart from their equilibrium values

given by (2.8) and (2.9). In particular, the minority carrier concentration can be easily overwhelmed by injection from neighboring regions. Under these circumstances, while the electrons and holes are in local equilibrium with themselves, they are not in equilibrium with each other. In order to extend the relationship between Fermi level and densities discussed above, we can introduce separate Fermi levels for electrons and holes. They are called *quasi Fermi levels* defined as E_{fn} and E_{fp} replacing equation (2.8) and (2.9):

$$n = n_i exp \left(\frac{E_{fn} - E_i}{k_B T} \right) \tag{2.18}$$

$$p = n_i exp \left(\frac{E_i - E_{fp}}{k_B T} \right) \tag{2.19}$$

In non equilibrium condition quasi Fermi levels have a similar physical interpretation in terms of the state occupancy as the Fermi level.

Observation 2.4. The electron density in the conduction band can be calculated using E_{fn}, and the hole density in the valence band using E_{fp}.

2.1.4 Carrier transport in semiconductor

Carrier transport or current flow in silicon is driven by two different mechanisms:

- the **drift** of carriers, which is caused by the presence of an electric field;

- the **diffusion** of carriers, which is caused by and electron or hole concentration gradient.

Drif current - Ohm's law

When an electric field is applied to a media, the free carriers are accelerated and acquire a drift velocity superimposed upon their random thermal motion.

Observation 2.5. The drift velocity of holes (h) is in the direction of the applied field, and the drift velocity of electrons (e) is opposite to the field.

The velocity of the carriers does not increase indefinitely under field acceleration, since they are scattered frequently and lose their acquired momentum after each collision. During their motion throughout the lattice structure, carriers travel at an average speed defnded as

$$\mathbf{v}_d^e = -\frac{q\mathbf{E}\tau_e}{m_e} \qquad \mathbf{v}_d^h = +\frac{q\mathbf{E}\tau_h}{m_h} \tag{2.20}$$

where $q = 1.602e^{-19}[C]$ is the elementary charge, $\mathbf{E}$ the electric field, τ_η the average time of flight of the carrier between two consecutive interactions with the atoms of the lattice and m_η is the effective mass. The coefficient $q\tau_\eta/m_\eta$ characterizes how quickly a carrier can move through the lattice and it's well known as carrier mobility $[m^2 V^{-1} s^{-1}]$. In general, to include different contributions to the mobility *Matthiessen's rule* is used:

$$\frac{1}{\mu} = \frac{1}{\mu_L} + \frac{1}{\mu_I} + \cdots \tag{2.21}$$

where μ_L and μ_I correspond to the lattice and impurity scattering limited components of mobility (for a more detailed description of mobility models see [YT09]).

Therefore the drift electron, hole, current density, reads as follows:

$$\mathbf{J}_n = - qn\mathbf{v}_d^n = qn\mu_n\mathbf{E} = \sigma_n\mathbf{E} \tag{2.22}$$

$$\mathbf{J}_p = + qp\mathbf{v}_d^p = qp\mu_p\mathbf{E} = \sigma_p\mathbf{E} \tag{2.23}$$

The scalar coefficient $qn\mu_n(qp\mu_p)$ is often summerized by the electron (hole) conductivity $\sigma_n(\sigma_p)$.

Relations (2.22) and (2.23) expresses the well known *Ohm' law* stating that the current density is directly proportional to the applied electric field.

Diffusion current - Fick's law

In semiconductor devices it's usual have different profiles of dopant in order to allow particular behaviors, this implies a not uniform concentration of carriers which they also diffuse as a result of the concentration gradient. This leads to an additional current contribution accordingly to the *Fick's law*:

$$\mathbf{J}_n = -D_n(-q\nabla n) \tag{2.24}$$

$$\mathbf{J}_p = -D_p(+q\nabla p) \tag{2.25}$$

The proportionally constants D_n and D_p are called the electron and hole diffusion coefficients and have units of $[cm^2 s^{-1}]$. Physically, both drift and diffusion are closely associated with the random thermal motion of carriers and their collisions with the silicon lattice in thermal equilibrium. A simple relationship between the diffusion coefficient and the mobility is the well known *Einstein relation*:

$$D_\eta = \frac{k_B T}{q}\mu_\eta \tag{2.26}$$

Drift-Diffusion transport equations

By considering (2.22), (2.23), (2.24) and (2.25), the total electron and hole current densities are:

$$\mathbf{J}_n = qn\mu_n\mathbf{E} + qD_n\nabla n \tag{2.27}$$

$$\mathbf{J}_p = qp\mu_p\mathbf{E} - qD_p\nabla p \tag{2.28}$$

The total conduction current density is $\mathbf{J} = \mathbf{J}_n + \mathbf{J}_p$.

We remark that these constitutive laws can be rewritten in two other ways highlighting different physical explanations of the same phenomenon. Moreover these reinterpreations give different start points for the discrete solver algorithm.

Considering that electric field is related to the scalar potential as:

$$\mathbf{E} = -\nabla\varphi \tag{2.29}$$

the current densities can be :

$$\mathbf{J}_n = -qn\mu_n\left(\nabla\varphi - \frac{k_BT}{qn}\nabla n\right)$$

$$\mathbf{J}_p = -qp\mu_p\left(\nabla\varphi + \frac{k_BT}{qp}\nabla p\right)$$

Considering equations (2.18) and (2.19) the above can be written as:

$$\mathbf{J}_n = -qn\mu_n\nabla\varphi_n \tag{2.30}$$

$$\mathbf{J}_p = -qn\mu_p\nabla\varphi_p \tag{2.31}$$

With these equations we underlying an important aspect which occur in semiconductor material:

Observation 2.6. The current density is proportional to the gradient of the quasi Fermi potential.

The third way to represent the current density is based on *Slotboom variables*. In 1973 Jan Slotboom proposed this change in variables for the two-dimensional numercal simulation of a bipolar transistor:

$$u_n = n_i exp\left(-\frac{\varphi_n}{V_{th}}\right) \tag{2.32}$$

$$u_p = n_i exp\left(\frac{\varphi_p}{V_{th}}\right) \tag{2.33}$$

where $V_{th} = k_B T / q$. Using the above equations into (2.27) and (2.28) we obtain:

$$\mathbf{J}_n = q D_n exp \left(\frac{\varphi}{V_{th}} \right) \nabla u_n \tag{2.34}$$

$$\mathbf{J}_p = -q D_p exp \left(-\frac{\varphi}{V_{th}} \right) \nabla u_p \tag{2.35}$$

This interpretation results is:

Observation 2.7. The drift-diffusion current density in a semiconductor, is a totally diffusive flux of a new kind of carrier and diffusivity coefficient.

2.2   Drift Diffusion Model for semiconductor

Simulations on integrated devices works on several different scale, the *Drift Diffusion model* (DD) is the most widely used mathematical tool for industrial simulaiton of semiconductor devices. In this section we'll show how is possible to deduce the DD model.

2.2.1   Drift Diffusion formulation

The system of Maxwell equations describes the propagation of electromagnetic signal in a medium:

$$\nabla \times \mathbf{H} = \mathbf{J} + \frac{\partial \mathbf{D}}{\partial t} \tag{2.36}$$

$$\nabla \times \mathbf{E} = -\frac{\partial \mathbf{B}}{\partial t} \tag{2.37}$$

$$\nabla \cdot \mathbf{D} = \rho \tag{2.38}$$

$$\nabla \cdot \mathbf{B} = 0 \tag{2.39}$$

we complete the system with the following set of constitutive laws that characterize the electromagnetic properties of the medium:

$$\begin{aligned} \mathbf{D} &= \epsilon \mathbf{E} \\ \mathbf{B} &= \mu_m \mathbf{H} \end{aligned} \tag{2.40}$$

where ϵ is the material dielectric permettivity $[F cm^{-1}]$ and μ_m is the magnetic permeability $[H cm^{-1}]$. Since $\nabla \cdot (\nabla \times \mathbf{A}) = 0$ for any vector $\mathbf{A}$,

(2.39) is satisfied by introducing a vector potential $\mathbf{A}$ such that $\mathbf{B} = \nabla \cdot \mathbf{A}$. We replace it in (2.37) and we obtain

$$\nabla \times \left(\mathbf{E} + \frac{\partial \mathbf{A}}{\partial t} \right) = 0. \tag{2.41}$$

From this we can state that exist a scalar potential φ such that

$$\mathbf{E} + \frac{\partial \mathbf{A}}{\partial t} = -\nabla \varphi \tag{2.42}$$

We multiply (2.42) by ϵ, we apply the divergence operator and we obtain using (2.29), (2.40) and (2.38)

$$\rho + \frac{\partial \mathbf{A}}{\partial t} = -\nabla \cdot (\epsilon \nabla \varphi) \tag{2.43}$$

We now assume that $\dfrac{\partial \mathbf{A}}{\partial t} = 0$ (quasi static approximation) and we obtain the *Poisson Equation*

$$\nabla \cdot (\epsilon \nabla \varphi) = \rho. \tag{2.44}$$

We apply the divergence operator on the equation [2.36] and we get the *Continuity Equation*

$$\frac{\partial \rho}{\partial t} + \nabla \cdot \mathbf{J} = 0 \tag{2.45}$$

To close the above system we need to specify the mathematical form of the electric charge density (ρ) and the electric conduction current density ($\mathbf{J}$). As we introduced in the preview section, devices are usually formed by extrinsic semiconductor and this causes the presence in the lattice of two kind of charge:

- free charge (ρ_{free}) (free electron and holes carriers),

- fixed charge (ρ_{fixed}) (ionoized dopant impurities).

$$\rho = \underbrace{q(p - n)}_{\rho_{free}} + \underbrace{q(N_D^+ - N_A^-)}_{\rho_{fixed}} \tag{2.46}$$

Notice that we assume N_D^+ and N_A^- time invariant ($\partial N_D^+ / \partial t = \partial N_A^- / \partial t = 0$).

Accordingly with the preview hypotesis and replacing (2.46), (2.27) and (2.28), we can split the continuity equation into the contribute of electrons and holes, the DD model formulation looks as follows:

$$
\begin{cases}
\nabla \cdot (-\epsilon \nabla \varphi) = q(p - n + N_D^+ - N_A^-) \\[2mm]
-q\dfrac{\partial n}{\partial t} + \nabla \cdot (-q\mu_n n \nabla \varphi + q D_n \nabla n) = qR \\[2mm]
q\dfrac{\partial p}{\partial t} + \nabla \cdot (-q\mu_p p \nabla \varphi - q D_p \nabla p) = -qR
\end{cases}
\tag{2.47}
$$

The system is an incompletely parbolic initial value/boundary problem in three scalar unkown dependent variables $\varphi(\mathbf{x}, t)$, $n(\mathbf{x}, t)$ and $p(\mathbf{x}, t)$. Notice that the problem is a nonlinearly coupled system of PDE's, because of the presence of the drift terms ($n\nabla\varphi$ and $p\nabla\varphi$).

From Maxwell equations we are able to guarantee only that $\mathbf{J}$ is a solenoidal field, we can't say nothing about the properties of $\mathbf{J_n}$ and $\mathbf{J_p}$. We can interpret $R(\mathbf{x}, t)$ as the net rate of generation and recombination.

The stationary form can be easily derivate from (2.47) by not considering the temporal derivative.

2.2.2   Generation and Recombination phenomenon

The modelling of $R(\mathbf{x}, t)$ is one of the most important feature due to the important role in determining the current-voltage characteristic of devices.

It's important to keep in mind that electrons and holes are in continuos fluctuation due to their thermal energy, but the macroscopic result of such a process at equilibrium is that the net recombination rate is identically zero at each point and at each time level. Therefore our interest is to analyze the deviations from this condition.

In every moment the system try to mantain the equilibrium, so it's important underlying that the response with a recombination event happens in order to neutralize an excess of charge, while generation event are usually due to thermal agitation or an external input source.

The phenomenological model for the net recombination rate R is often given by the sequent formulation:

$$
R(n, p) = (pn - n_i^2)F(n, p)
\tag{2.48}
$$

where F is a function modelling the specific recombination/generation (R/G) event.

In the following we present the classical theory about three kind of contribute.

Shockley-Read-Hall recombination (SRH)

Electron and hole generation and recombination can take place directly between the valence band and the conduction band, or inderactly via trap centers in the energy gap (we indicate with E_T the energy level at where these traps live). The latter category includes Shockley-Read-Hall phenomena (SRH), more precisely SRH rate is a two-particle process which matematically expresses the probality that:

R_{SRH} an electron in the conduction band neutralizes a hole at the valence band through the mediation of an unoccupied trapping level located in the energy gap,

G_{SRH} an electron is emitted from the valence band to the conduction band, through he mediation of an unoccupied trapping level located in the energy gap.

The following expression is usually employed for the modulating function F:

$$F_{SRH}(n,p) = \frac{1}{\tau_n \left(p + n_i cosh \left(\frac{E_T}{k_B T} \right) \right) + \tau_p \left(n + n_i cosh \left(\frac{E_T}{k_B T} \right) \right)} \quad (2.49)$$

the quantiaties τ_n and τ_p are called *carrier lifetimes* and are phisically defined as the reciprocals of the capture rates per single carrier associated with the energy trap distribution within the semiconductor energy gap. Their typical order of magnitude lies in the range $10^{-3}\mu s \div 1\mu s$.

Parameter	Unit	Electrons	Holes
τ	s	1.0×10^{-5}	3.0×10^{-6}
E_T	eV	0.0	0.0

Tabella 2.1: List of parameters in the electron and hole mobility models including scattering from lattice thermal vibrations

Auger recombination (AU)

Auger R/G is a three-particle process and take place directly between the valence band and the conduction band. We distinguish four cases which depend to the kind of carriers involved in the phenomena:

$R_{AU}^{2n,1p}$ a high-energy electron in the conduction band moves to the valence band where it neutralizes a hole, transmitting the excess energy to another electron in the conduction band;

$G_{AU}^{2n,1p}$ an electron in the valence band moves to the conduction band by taking the energy from a high energy electron in the conduction band and leaves a hole in the valence band;

$R_{AU}^{2p,1n}$ an electron in the conduction band moves to the valence band where it neutralizes a hole, transmitting the excess energy to another hole in the valence band;

$G_{AU}^{2p,1n}$ an electron in the valence band moves to the conduction band by taking the energy from a high energy hole in the valence band and leaves a hole in the valence band.

The following expression is usually employed for the modulating function F:

$$F_{AU}(n,p) = C_n n + C_p p \qquad (2.50)$$

where the quantitaties C_n and C_p are the so called Auger capture coefficients tipically of the order of magnitude of $10^{-25} [cm^6 s^{-1}]$. Note that Auger R/G is relevant only when both carrier densities attain high values.

Parameter	Unit	Magnitude
C_n	$cm^6 s^{-1}$	2.9×10^{-31}
C_p	$cm^6 s^{-1}$	1.028×10^{-31}

Tabella 2.2: List of parameters in the electron and hole Auger generation/recombination model.

Impact ionization (II)

The impact ionization mechanism is a three-particle generation process and it is dissimilar from the previously phenomenon because we can't express its

contribute with a relation like (2.48). The high energy carrier generation is triggered by the presence of very high electric fields. Due to these fields an electron could gains enough energy to excite an electron-hole pair out of a silicon lattice bond. Then the process can be repeated until an avalanche of generated carriers is produced within the region. There are several different models for the II generation, inside our code we implemented the van Overstraeten - de Man referenza manuale sdevice model based on the Chynoweth law referenza dentro sdevice:

$$G_{II}(n,p) = \alpha_n n |\mathbf{v}_n| + \alpha_p p |\mathbf{v}_p| \tag{2.51}$$

where:

$$\alpha(E_{ava}) = \gamma exp\left(-\frac{\gamma b}{E_{ava}}\right) \tag{2.52}$$

$$\gamma = \frac{tanh\left(\dfrac{\hbar\omega_{op}}{2k_B T_0}\right)}{tanh\left(\dfrac{\hbar\omega_{op}}{2k_B T}\right)} \tag{2.53}$$

The factor γ with the optical phono energy $\hbar\omega_{op}$ expresses the temperature dependence of the phonon gas against which carriers are accelerated. E_{ava} is the driving force which takes into account how the electric field influence the generation event. There are two possibilties to compute this quantity:

- compute the component of the elctrostatic field in the direction of the current

$$E_{ava}^{n,p} = \frac{\mathbf{E} \cdot \mathbf{J}_{n,p}}{||\mathbf{J}_{n,p}||} \tag{2.54}$$

- consider the module of the quasi fermi gradient

$$E_{ava}^{n,p} = |\nabla\varphi_{n,p}| \tag{2.55}$$

2.2.3 Mobility models

In the following section we illustrate the most commonly used phenomenological models to describe carrier mobilities. More precisely we want describe the several mechanisms that characterize the average time of flight (2.20). Scattering phenomenon slow down the motion of carriers throughout the lattice and the three main physical principles governing these events are:

Parameter	Unit	Electrons	Holes	Valid range of electric field
E_0	$V\,cm^{-1}$	4.0×10^5	4.0×10^5	
a_{high}	1	7.03×10^5	6.71×10^5	E_0 to 6.0×10^5
a_{low}	1	7.03×10^5	1.582×10^6	1.75×10^5 to E_0
b_{high}	1	1.231×10^6	1.693×10^6	E_0 to 6.0×10^5
b_{low}	1	1.231×10^6	2.036×10^6	1.75×10^5 to E_0
$\hbar\omega_{op}$	eV	0.063	0.063	

Tabella 2.3: List of parameters in the electron and hole of van Overstraeten-de Man model

Parameter	Unit	Electrons	Holes
μ^0	$cm^2 V^{-1} s^{-1}$	1417.0	470.5
β	1	2.5	2.2

Tabella 2.4: List of parameters in the electron and hole mobility models including scattering from lattice thermal vibrations

- interaction with the thermally generated vibrations of the silicon atoms;

- presence of ionized dopant impurities in the crystal;

- reduction to the velocity saturation at high electric fields.

Scattering from thermal vibrations

Intuitively, carrier mobility is to be a decreasing function of temperature, as we expect collisions to become more and more frequent as T gets higher. This idea is commonly represented using a simple power law of the form

$$\mu_\nu^L = \mu_\nu^0 \left(\frac{T}{T_0}\right)^{-\beta_\nu} \qquad \nu = n, p \tag{2.56}$$

where μ_ν^0 is the low-field mobility, β_ν are positive numbers and T_0 is a reference temperature typically $T_0 = 300[K]$.

Scattering from Ionized Impurities

Dopant ionized impurities represent local perturbations of the periodic distribution of silicon atoms. They strongly influence the carrier motion through electrostatic interaction, reducing the mobility of electrons and holes. The

model used to simulate doping-dependent mobility in silicon was proposed by *Masetti*:

$$\mu = \mu_{min1} exp\left(-\frac{P_c}{N_{tot}}\right) + \frac{\mu^L - \mu_{min2}}{1 + \left(\frac{N_{tot}}{C_r}\right)^\alpha} - \frac{\mu_1}{1 + \left(\frac{C_s}{N_{tot}}\right)^\beta} \qquad (2.57)$$

where $N_{tot} = N_D^+ + N_A^-$, μ_ν^L is given by (2.56), μ_{min1} and μ_{min2} are a positive quantities representing the minimum value of μ, P_c, C_r and C_s are reference doping values.

Parameter	Unit	Electrons	Holes
μ_{min1}	$cm^2V^{-1}s^{-1}$	52.2	44.9
μ_{min2}	$cm^2V^{-1}s^{-1}$	52.2	0
μ_1	$cm^2V^{-1}s^{-1}$	43.4	29.0
P_c	cm^{-3}	0	9.23×10^{16}
C_r	cm^{-3}	9.68×10^{16}	2.23×10^{17}
C_s	cm^{-3}	3.43×10^{20}	6.10×10^{20}
α	1	0.680	0.719
β	1	2.0	2.0

Tabella 2.5: List of parameters in the electron and hole mobility models including scattering from ionized dopant impurities.

Veclocity saturation at high electric field

Under the assumption of low electric field, mobilities are reasonably constant and the carrier drift velocity is proportional to the electric field. As the applied field strength increases, the above assumption is completely wrong as it would predict an unbounded carrier velocity in the material as $|\mathbf{E}| \to \infty$. On the contrary, carrier scattering with lattice phonos produces a limitation to carrier velocity according to the following mathematical expression

$$\lim_{|\vec{E}|\to\infty} \mu|\mathbf{E}| = v_{sat} \qquad (2.58)$$

A common adopted formula is the *Canali model* with temperature dependent parameters

$$\mu = \frac{\mu_L}{\left[1 + \left(\dfrac{\mu_L |\mathbf{E}|}{v_{sat}}\right)^{\beta}\right]^{1/\beta}} \tag{2.59}$$

$$v_{sat} = v_0 exp\left(\frac{300}{T}\right)^{v_{exp}} \qquad \beta = \beta_0 \left(\frac{T}{300}\right)^{\beta_{exp}}. \tag{2.60}$$

Parameter	Unit	Electrons	Holes
v_0	$cm\ s^{-1}$	1.07×10^7	8.37×10^6
v_{exp}	1	0.87	0.52
β_0	1	1.109	1.213
β_{exp}	1	0.66	0.17

Tabella 2.6: List of parameters in the electron and hole mobility models including scattering from velocity saturation.

Capitolo 3

Resolution of the system

The aim of this chapter is to introduce notation and to present the physical model exposed in the previous chapter, in a more precisely and mathematical form. A briefly overview on the avaible and used iteration algorithms is then treated.

3.1 Geometry and boundary conditions

Consider the stationary form of problem (2.47), in order to proceed we have to close the *Poisson equation* and the *Drift Diffusion equation* for electrons and holes with suitable boundary conditions over the domain.

Let us consider the device domain as the union of two open disjoint subsets, Ω_{Si} (doped silicon part), and Ω_{ox} (oxide part), such that their intersection $\partial\Omega_{Si} \cap \partial\Omega_{ox} = \Gamma_{int}$ is the interface. The oxide region Ω_{ox} is assumed to be a perfect insulator so that:

$$
\begin{aligned}
n = p = 0 \\
\mathbf{J}_n = \mathbf{J}_p = \mathbf{0}
\end{aligned}
\tag{3.1}
$$

The device boundary $\partial\Omega$ is divided into two disjoint subsets: $\partial\Omega_c$ and $\partial\Omega_a$. The subset $\partial\Omega_c$ includes the so called *ohmic contacts*. With ohmic contacts we define every electrical terminal of the device on which the external input voltages are applied. Moreover ohmic contacts are assumed to be *ideal*, they are equipotential surfaces and no voltage drop occurs at the interface between the contact and the neighbouring material. This event is well performed by suitable Dirichlet boundary conditions, therefore in the follow we indicate $\partial\Omega_c = \Gamma_D$.

$$\begin{aligned} \varphi &= \varphi_D \\ n &= n_D \qquad on\, \Gamma_D. \\ p &= p_D \end{aligned} \qquad (3.2)$$

In the case where the neighbouring material is a perfect insulator, hypotesis (3.1) takes in place and therefore no Drift-Diffusion equations are solved, this implies that (3.2) reduces to the sole condition on the potential.

Artificial boundaries $(\partial\Omega_a)$ are needed in order to obtain a self-contained simulaiton domain. On these boundaries no electric and current flux is exchanged with the surrounding enviroment, this fact is well performed by homogeneous Neumann boundary condition $(\partial\Omega_a = \Gamma_N)$

$$\begin{aligned} \mathbf{D} \cdot \mathbf{n} &= 0 \\ \mathbf{J}_n \cdot \mathbf{n} &= 0 \qquad on\, \Gamma_N \\ \mathbf{J}_p \cdot \mathbf{n} &= 0 \end{aligned} \qquad (3.3)$$

where $\mathbf{n}$ is the outward unit normal vector defined over $\partial\Omega$. As we noted before on $\partial\Omega_{ox} \cap \Gamma_N$ condition (3.3) reduces to the sole one related with the Poisson equation.

Finally when we solve a Drift-Diffusion equation, if $\Omega_{ox} \neq \varnothing$ boundary shape could be change. Although the treatment of boundaries doesn't change
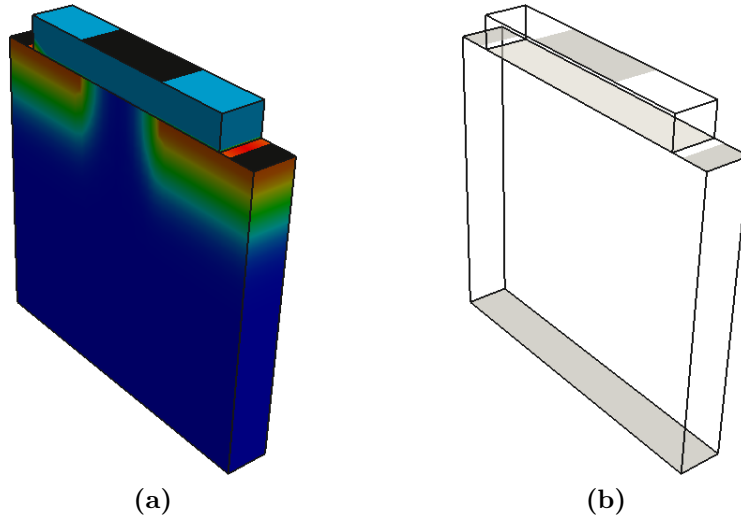

(a)   (b)

Figura 3.1: (a) Mos device with net dopant concentration distributed accordingly to a gaussian profile and Γ_D colored in black. The oxide layer is colored in light blue. (b) Outline of the Mos device with Γ_{int} in light gray.

if you consider the suitable restrictions and extensions

$$\begin{aligned}
\Gamma_{D,Si} &= \Gamma_D \cap \partial\Omega_{Si} \\
\Gamma_{N,Si} &= \Gamma_N \cap \partial\Omega_{Si} \cup \Gamma_{int}.
\end{aligned} \tag{3.4}$$

In silicon material the ideal condition on contacts is accomplished if both thermodynamical equilibrium and charge neutrality are reached. These two conditions correspond to the following algebraic system for n_D and p_D

$$\begin{cases} p_D n_D &= n_i^2 \\ p_D - n_D + N_D - N_A &= 0 \end{cases} . \tag{3.5}$$

Solving (3.5) on $\Gamma_{D,Si}$ we obtain:

$$n_D = \frac{D + \sqrt{D^2 + 4n_i^2}}{2} \tag{3.6}$$

$$p_D = \frac{-D + \sqrt{D^2 + 4n_i^2}}{2} \tag{3.7}$$

where $D := N_D - N_A$ is the net doping concentration. Furthermore we can approximate that quasif fermi potential level of silicon at contact is aligend with the external applyed voltage. As a conseguence we can easily calculate potential condition on $\Gamma_{D,Si}$ using (2.8) and (2.9)

$$\varphi_D = \varphi_f + V_{th} ln\left(\frac{n_D}{n_i}\right) = \varphi_f - V_{th} ln\left(\frac{p_D}{n_i}\right) \tag{3.8}$$

where $\varphi_f = -E_f/q$ is the unique quasi fermi potential level defined on contacts. When $\Omega_{ox} \neq \varnothing$ we set φ_D equal to the external applyed voltage on $\Gamma_D/\Gamma_{D,Si}$.

As we conveyed the boundary conditions, we are able to write in the closed way the stationary form of problem (2.47) as follows:

$$\begin{aligned}
-\Delta\epsilon\varphi - qn_i(e^{((\varphi_p-\varphi)/V_{th})} - e^{((\varphi-\varphi_n)/V_{th})}) &= qD & in\,\Omega = \Omega_{ox} \cup \Omega_{Si} \\
\varphi &= \varphi_D & on\,\Gamma_D \\
\nabla\varphi \cdot \mathbf{n} &= 0 & on\,\Gamma_N
\end{aligned}$$

$$\begin{aligned}
\nabla \cdot (q\mu_n n\nabla\varphi - qD_n\nabla n) &= -qR & in\,\Omega_{Si} \\
n &= n_D & on\,\Gamma_{D,Si} \\
\nabla n \cdot \mathbf{n} &= 0 & on\,\Gamma_{N,Si}
\end{aligned}$$

$$\begin{aligned}
\nabla \cdot (-q\mu_p p\nabla\varphi - qD_p\nabla p) &= -qR & in\,\Omega_{Si} \\
p &= p_D & on\,\Gamma_{D,Si} \\
\nabla p \cdot \mathbf{n} &= 0 & on\,\Gamma_{N,Si}
\end{aligned}$$

$$\tag{3.9}$$

The high coupled nonlinear nature of system (3.9) makes an analytical treatment very difficult, if not even impossible. For this reason, numerical schemes must be used to compute an approximate solution.

3.2   Iteration algorithms

The most used algorithms are *the fully coupled Newton's method* and *the decoupled Gummel map*. First of all we introduce a more compact form of (3.9):

$$\mathbf{F}(\mathbf{U}) = \mathbf{0} \tag{3.10}$$

where:

$$\mathbf{U} := [\varphi, n, p]^T \qquad \mathbf{F}(\mathbf{U}) := \begin{bmatrix} F_1(\mathbf{U}) \\ F_2(\mathbf{U}) \\ F_3(\mathbf{U}) \end{bmatrix} \tag{3.11}$$

and having set:

$$F_1(\mathbf{U}) = \nabla \cdot (-\epsilon \nabla \varphi) - q(n_i(e^{((\varphi_p - \varphi)/V_{th})} - e^{((\varphi - \varphi_n)/V_{th})}) + D)$$
$$F_2(\mathbf{U}) = \nabla \cdot (q\mu_n n \nabla \varphi - qD_n \nabla n) + qR$$
$$F_3(\mathbf{U}) = \nabla \cdot (-q\mu_p p \nabla \varphi - qD_p \nabla p) + qR$$

The non linear problem (3.10) is the abstract generalization of the search of a zero for a real function $f : \mathbb{R} \to \mathbb{R}$. The vector function $\mathbf{F}$ is a nonlinear differential operator and the associated problem which we intend to resolve is: given a functional space V and the operator $\mathbf{F} : V \to V$, find $\mathbf{U} \in V$ such that (3.10) is satisfied.

In our application, the function space V is tipycally a subset of the Sobolev space $[H^1(\Omega)]^d$ (in this case with d we intend the number of component of $\mathbf{F}$). Sobolev spaces are based on the space of square integrable functions on Ω which reads as follows

$$L^2(\Omega) := \left\{ v : \int_\Omega |v|^2 d\Omega = ||v||^2_{L^2(\Omega)} < +\infty \right\}. \tag{3.12}$$

The general form of a Sobolev space for an integer $m \geq 0$ is

$$H^m(\Omega) := \left\{ v : D^\alpha v \in L^2(\Omega), \forall |\alpha| \leq m \right\}. \tag{3.13}$$

On this space, we shall use the semi-norm

$$|v|^2_{m,\Omega} = \sum_{|\alpha|=m} ||D^\alpha v||^2_{L^2(\Omega)} \tag{3.14}$$

and the norm

$$||v||^2_{m,\Omega} = \sum_{k\leq m} |D^\alpha v|^2_{k,\Omega} \tag{3.15}$$

We shall also need to consider functions that vanish on either the entire or a part of the boundary

$$H^1_0 := \left\{ v : v \in H^1(\Omega), v|_{\partial\Omega} = 0 \right\} \tag{3.16}$$

$$H^1_{0,\Gamma_D} := \left\{ v : v \in H^1(\Omega), v|_{\Gamma_D} = 0 \right\} \tag{3.17}$$

For $v \in H^1_0(\Omega)$ we have the *Poincaré inequality*

$$|v|_{0,\Omega} \leq C(\Omega)|v|_{1,\Omega} \tag{3.18}$$

and the seminorm $|\cdot|_\Omega$ is therefore a norm in $H^1(\Omega)$, equivalent to $||\cdot||_{1,\Omega}$.

The above setting of function spaces are used widely in the proceeding of this work.

3.2.1 Abstract Newton's method

Before introducing the abstract Newton's method we have to define some useful concept.

Definition 3.1 (Frechèt derivative)**.**

Definition 3.2 (Jacobian matrix)**.** Given a vector function $\mathbf{F}$ the Jacobian matrix $\mathbf{F}'$

Accordingly with the above definitions the abstract Newton's method reads as follows:

Newton's method

Let be $\mathbf{F}$ a function operator, given $\mathbf{U}^0 \in V$, for all $k \geq 0$ until convergence, solve the following linearized problem:

$$\begin{aligned} \mathbf{F}'(\mathbf{U}^k)\delta\mathbf{U}^k &= -\mathbf{F}(\mathbf{U}^k) \\ \mathbf{U}^{k+1} &= \mathbf{U}^k + \delta\mathbf{U}^k \end{aligned} \tag{3.19}$$

The application of Newton's method has transformed the original problem
(3.10) into the *fixed-point problem* of finding $\mathbf{U} \in V$ such that

$$\mathbf{U} = T_{\mathbf{F}}(\mathbf{U}) \tag{3.20}$$

where

$$T_{\mathbf{F}}(\mathbf{U}) = \mathbf{F}'(\mathbf{U})^{-1}(\mathbf{F}'(\mathbf{U})\mathbf{U} - F(\mathbf{U})) \tag{3.21}$$

is the *iteration function* associated with the Newton method. Here we
present the main result about the convergence of this method.

Theorem 3.1. *Let $\mathbf{U} \in V$ be a solution of problem (3.10). Assume that $\mathbf{F}'$
is Lipschitz continuos in the ball $\mathcal{B}(\mathbf{U}, \delta)$, i.e., that there exists $K > 0$ such
that:*

$$||\mathbf{F}'(\mathbf{v}) - \mathbf{F}'(\mathbf{z})||_{L(V,V)} \leq K||\mathbf{v} - \mathbf{z}||_V \qquad \forall \mathbf{v}, \mathbf{z} \in \mathcal{B}(\mathbf{U}, \delta), \mathbf{v} \neq \mathbf{z} \tag{3.22}$$

*Then there exists in correspondence $\delta' > 0$, with $\delta' \leq \delta$, such that for all
$\mathbf{U}^0 \in \mathcal{B}(\mathbf{U}, \delta')$ the sequence $\{\mathbf{U}^k\}$ generated by (3.19) converges quadratically
to $\mathbf{U}$, i.e., there exists $C > 0$ such that, for a suitable $k_0 \geq 0$ we have:*

$$||\mathbf{U} - \mathbf{U}^{k+1}||_V \leq C||\mathbf{U} - \mathbf{U}^k||_V^2 \qquad \forall k \geq k_0 \tag{3.23}$$

3.2.2   Fully coupled Newthon's method

If we consider the linearization of the entire system (3.9) the relative Jacobian
matrix is a 3x3 matrix of the form

$$\begin{bmatrix} F_{1,\varphi} & F_{1,n} & F_{1,p} \\ F_{2,\varphi} & F_{2,n} & F_{2,p} \\ F_{3,\varphi} & F_{3,n} & F_{3,p} \end{bmatrix} \begin{bmatrix} \delta\varphi \\ \delta n \\ \delta p \end{bmatrix} = \begin{bmatrix} -F_1(\varphi, n, p) \\ -F_2(\varphi, n, p) \\ -F_3(\varphi, n, p) \end{bmatrix}. \tag{3.24}$$

Every entry of the above matrix is a PDE's equation which we can di-
scretize with suitable numerical proceedings (i.e. finite element method). If
we spent for example N_{dof} degrees of freedom to represent $\delta\varphi$, δn and δp
we note that the structure of the relative discretizated matrix is a 3x3 block
matrix system where every block is a $N_{dof} \times N_{dof}$ matrix:

$$\begin{bmatrix} \mathbf{K}_{1,\varphi} & \mathbf{K}_{1,n} & \mathbf{K}_{1,p} \\ \mathbf{K}_{2,\varphi} & \mathbf{K}_{2,n} & \mathbf{K}_{2,p} \\ \mathbf{K}_{3,\varphi} & \mathbf{K}_{3,n} & \mathbf{K}_{3,p} \end{bmatrix} \begin{bmatrix} \delta\varphi \\ \delta n \\ \delta p \end{bmatrix} = \begin{bmatrix} -\mathbf{F}_1(\varphi, n, p) \\ -\mathbf{F}_2(\varphi, n, p) \\ -\mathbf{F}_3(\varphi, n, p) \end{bmatrix}. \tag{3.25}$$

This implies that at every iteration step we have to solve a linear problem
of $3 \times N_{dof}$ dimension ...

Moreover to ensure convergence of the Newton iterative process, it is particularly important to provide a very good initial guess vector $[\varphi_0, n_0, p_0]$, therefore we have to know for every equation a possibly shape of the solution.

Finally variable in play have different order of magnitude and the jacobian matrix is often quite ill-conditioned and needs appropriate scaling and balancing in order to avoid problems associated with round-off error.

This method is widely used in commercial software especially for the strong result ...

3.2.3 Gummel map algorithm

In 1964 H. K. Gummel proposed an orginal and alternative iterative algorithm in order to solve the system (3.9) in a semiconductor device in one spatial dimension.

The main idea of the algorithm is to move the nonlinearity to the Poisson equation only and once obtained the electric potential profile, both continuity equations are linearized. More precisely give an initial guess for φ, n and p, the functional iteration consists in the succesive solution of the nonlinear Poisson's equation (NLP) in a inner loop (Newton's method is applyed for this equation) and of the two linearized continuity equations (DD electrons and DD holes). A concisely scheme is presented in Fig.3.2.

Unfortunately there isn't any convergence result for this method like (3.1), although there are several advantages which make Gummel map algorithm preferable to the Fully Coupled Newton's Method. In fact simulations experience shows that the Gummel process is much more insesitive to the choice of the initial guess than Newton's method. This is particularly important in multidimensional problems where it is far from trivial to design a good starting point for initializing.

Another attractive feature is the reduced computational and memory stage cost: at each iteration step the Gummel algorithm requires the successive solution of three problems, each one of size equal to $N_{dof} \times N_{dof}$.

(Step 0) Give a suitable initial condition for φ_i^0 n^0 and p^0.

(Step 1) Fixed a positive parameter $toll > 0$, solve the linearized Non Linear Poisson equation (NLP) in Ω using the Newton's method untill $||F_1(\varphi_i^{k+1})|| > toll$:

$$\begin{cases} \nabla \cdot (-\epsilon_{Si} \nabla \delta\varphi^k) + \dfrac{1}{V_{th}} \sigma_{Si}^k \delta\varphi^k = f_{Si}^k & in \ \Omega_{Si} \\ \nabla \cdot (-\epsilon_{ox} \nabla \delta\varphi^k) = f_{ox}^k & in \ \Omega_{ox} \\ \delta\varphi^k = 0 & on \ \Gamma_D \\ \nabla\delta\varphi^k \cdot \mathbf{n} = 0 & on \ \Gamma_N \\ \varphi^{k+1} = \varphi^k + \delta\varphi^k \end{cases} \tag{3.26}$$

having set,

$$\sigma_{Si}^k(\varphi^k, \varphi_n^i, \varphi_p^i) = qn_i \left[e^{((\varphi_p^i - \varphi^k)/V_{th})} - e^{((\varphi^k - \varphi_n^i)/V_{th})} \right]$$

$$f_{Si}^k(\varphi^k, \varphi_n^i, \varphi_p^i) = \nabla \cdot (-\epsilon \nabla\varphi^k) + qn_i \left[e^{((\varphi_p^i - \varphi^k)/V_{th})} - e^{((\varphi^k - \varphi_n^i)/V_{th})} + D \right]$$

$$f_{ox}^k(\varphi^k) = \nabla \cdot (-\epsilon \nabla\varphi^k)$$

(Step 2) Solve the Linear Electron Contintuity Equation (LEC):

$$\begin{cases} \nabla \cdot (q\mu_n n \nabla\varphi^i - qD_n \nabla n) = -qR(n^{i-1}, p^{i-1}) & in \ \Omega_{Si} \\ n = n_D & on \ \Gamma_{D,Si} \\ \nabla n \cdot \mathbf{n} = 0 & on \ \Gamma_{N,Si} \end{cases} \tag{3.27}$$

(Step 3) Solve the Linear Hole Contintuity Equation (LHC):

$$\begin{cases} \nabla \cdot (-q\mu_p p \nabla\varphi^i - qD_p \nabla p) = -qR(n^{i-1}, p^{i-1}) & in \ \Omega_{Si} \\ p = p_D & on \ \Gamma_{D,Si} \\ \nabla p \cdot \mathbf{n} = 0 & on \ \Gamma_{N,Si} \end{cases} \tag{3.28}$$

(Step 4) If $max\{||\varphi^i - \varphi^{i-1}||_{L^\infty}, ||p^i - p^{i-1}||_{L^\infty}, ||n^i - n^{i-1}||_{L^\infty}\} > toll$ restart from step 1.

We spent some considerations over step 2 and step 3. The general recombination/generation phenomenon is described by (2.48), this implies that we can separate the reaction term from the force term (except for the II which is only a force term contribution). In fact we can denote the general recombination/generation term as follows:

$$\begin{aligned} R_n^{i-1}(n) &= \sigma_n^{i-1} n - f^{i-1} \\ R_p^{i-1}(p) &= \sigma_p^{i-1} p - f^{i-1} \end{aligned} \tag{3.29}$$

where

$$\sigma_n = \frac{p^{i-1}}{F(p^{i-1}, n^{i-1})} \qquad \sigma_p = \frac{n^{i-1}}{F(p^{i-1}, n^{i-1})}$$

$$f = \frac{n_i^2}{F(p^{i-1}, n^{i-1})}. \tag{3.30}$$

We can rewrite systems (3.27) and (3.28)

$$\begin{cases} \nabla \cdot (q\mu_n n \nabla \varphi^i - q D_n \nabla n) + q \sigma_n^{i-1} n = q f^{i-1} & in \ \Omega_{Si} \\ n = n_D & on \ \Gamma_{D,Si} \\ \nabla n \cdot \mathbf{n} = 0 & on \ \Gamma_{N,Si} \end{cases} \tag{3.31}$$

$$\begin{cases} \nabla \cdot (-q\mu_p p \nabla \varphi^i - q D_p \nabla p) + q \sigma_p^{i-1} p = q f^{i-1} & in \ \Omega_{Si} \\ p = p_D & on \ \Gamma_{D,Si} \\ \nabla p \cdot \mathbf{n} = 0 & on \ \Gamma_{N,Si} \end{cases} \tag{3.32}$$

We just introduced a special treatment of the continuity equations in the Gummel Decoupled Algorithm. This splitting of R/G term is called *lagging approach* and corresponds to extending to the non-linear case the classical *Jacobi* method for the iterative solution of linear algbraic systems. Thus equations are sequentially solved, it's possible take advantage of the knowing a solution. Indeed an alternative approach would be use the solution of the first solved equation to compute the R/G contribute in the second equation. In such case the lagging method corresponds to extending to the nonlinear case tha classical *Gauss-Seidel* method for the iterative solution in linear algebraic systems.
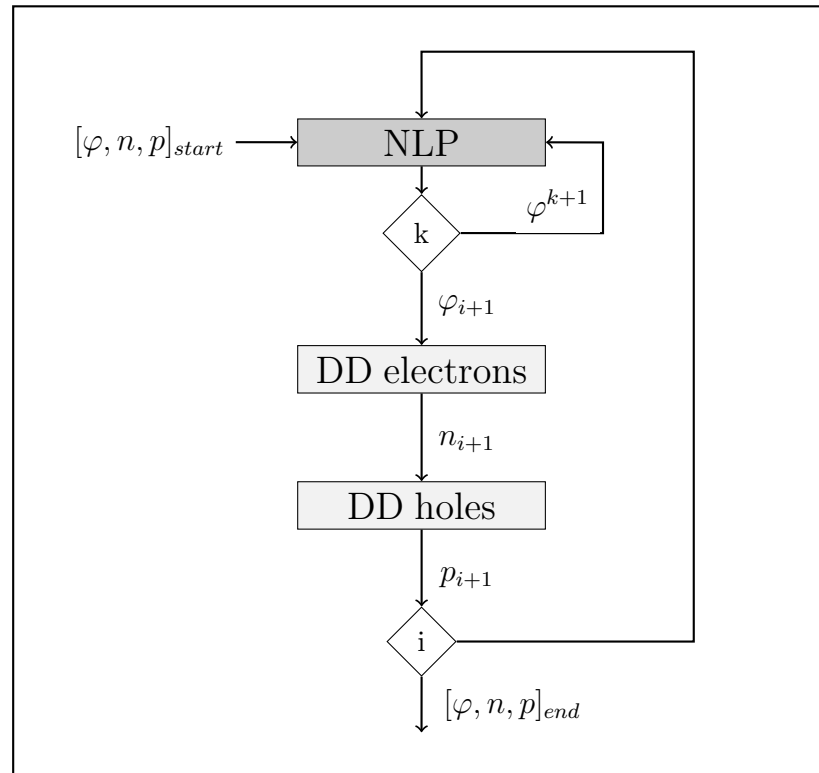
Figura 3.2: Gummel map algorithm

Capitolo 4

Finite element discretization

In this section we shall present the classical variational formulation of problems (3.26), (3.31) and (3.32). For each kind of PDE problem we give a briefly presentation of the well-posedness analysis. Finally we describe the finite element discretization.

4.1 Non Linear Poisson Equation weak form

Let us write problem (3.26) in a more compact form

$$\begin{cases} \nabla \cdot (-\epsilon \nabla \delta \varphi^k) + \sigma^k \delta \varphi^k & = & f^k & in \ \Omega \\ \delta \varphi^k & = & 0 & on \ \Gamma_D \\ \nabla \delta \varphi^k \cdot \mathbf{n} & = & 0 & on \ \Gamma_N \\ \varphi^{k+1} & = & \varphi^k + \delta \varphi^k \end{cases} \qquad (4.1)$$

having set

$$\epsilon = \epsilon_s \mathcal{I}_{\Omega_{Si}} + \epsilon_{ox} \mathcal{I}_{\Omega_{ox}}$$
$$f = f_s \mathcal{I}_{\Omega_{Si}} + f_{ox} \mathcal{I}_{\Omega_{ox}}$$
$$\sigma = \sigma_s \mathcal{I}_{\Omega_{Si}}$$

where $\mathcal{I}_A(\mathbf{x})$ is equal to 1 if $\mathbf{x} \in A$ and 0 otherwise. System (4.1) constitute a classical Diffusion-Reaction (DR) problem in Ω, respect the variable $\delta \varphi^k$. Now we multiply the equation with a test function $v \in H^1_{\Gamma_D}$ and we integrate over all the domain

$$-\int_\Omega \epsilon \Delta \delta \varphi^k v \, d\Omega + \int_\Omega \sigma^k \delta \varphi^k v \, d\Omega = \int_\Omega f^k v \, d\Omega \qquad \forall v \in H^1_{\Gamma_D}(\Omega). \quad (4.2)$$

35

Applying the Green-formula on (4.2) and then considering the boundary conditions, we get the weak formulation which reads as: find $\delta\varphi^k \in H^1_{\Gamma_D}(\Omega)$ such that

$$\int_\Omega \epsilon\nabla\delta\varphi^k\nabla v\,d\Omega + \int_\Omega \sigma^k\delta\varphi^k v\,d\Omega = \int_\Omega f^k v\,d\Omega \qquad \forall v \in H^1_{\Gamma_D}(\Omega) \qquad (4.3)$$

We are able to define the following bilinear form

$$a : H^1_{\Gamma_D}(\Omega) \times H^1_{\Gamma_D}(\Omega) \to \mathbb{R}, \qquad a(u,v) = \int_\Omega \epsilon\nabla u\nabla v\,d\Omega + \int_\Omega \sigma^k uv\,d\Omega \quad (4.4)$$

and the linear and bounded functional

$$F : H^1_{\Gamma_D}(\Omega) \to \mathbb{R}, \qquad F(v) = \int_\Omega f^k v\,d\Omega \qquad\qquad (4.5)$$

In order to prove the existence and uniqueness of the solution, we apply the *Lax-Millgram theorem* [Sal10] to the weak formulation (4.3). The well-posedness is ensured by several and physical hypotesis:

- $\epsilon \in L^\infty(\Omega)$ and $\exists m$ s.t. $0 < m \leq \epsilon$ (a.e.) in Ω;

- $\forall k \geq 0$ $\sigma^k \in L^\infty(\Omega)$ and $\exists m$ s.t. $0 < m \leq \sigma^k$ (a.e.) in Ω_{Si}.

We define some useful quantities:

$$\epsilon_M = max_\Omega\epsilon \quad \epsilon_m = min_\Omega\epsilon$$
$$\sigma_M = max_\Omega\sigma \quad \sigma_m = max_\Omega\sigma = 0$$

Take into account the above hypotesis one can demonstrate:

- **Continuity of the bilinear form**,

  $\forall u, v \in H^1_{\Gamma_D}$

  $$\begin{aligned}
  \left|\int_\Omega \epsilon\nabla u\nabla v + \int_\Omega \sigma^k uv\right| &\leq \epsilon_M||\nabla u||_{L^2}||\nabla v||_{L^2} + \sigma_M||u||_{L^2}||v||_{L^2} \\
  &\leq max\{\epsilon_M, \sigma_M\}\left(||\nabla u||_{L^2}||\nabla v||_{L^2} + ||u||_{L^2}||v||_{L^2}\right) \\
  &\leq max\{\epsilon_M, \sigma_M\}||u||_{H^1_{\Gamma_D}}||v||_{H^1_{\Gamma_D}}
  \end{aligned}$$

- **Coercivity of the bilinear form**,

  $\forall u \in H^1_{\Gamma_D}$

  $$\begin{aligned}
  \left|\int_\Omega \epsilon\nabla u\nabla u + \int_\Omega \sigma^k u^2\right| &\geq \epsilon_m||\nabla u||^2_{L^2} + \sigma_m||u||^2_{L^2} \\
  &= \epsilon_m||\nabla u||^2_{L^2} \\
  &= \epsilon_m|\nabla u|^2_{H^1_{\Gamma_D}}
  \end{aligned}$$

- **Continuity of the functional,**

$$| \int_\Omega f^k v | \ \leq ||f^{(k)}||_{L^2} ||v||_{L^2} \qquad \forall v \in H^1_{\Gamma_D}$$

Then we can state that $\forall k \geq 0$ there exists a unique solution of the linearized Non Linear Poisson equation.

4.2 Continuity Equations weak form

Without loss of generality we can consider only the electron continuity equation. System (3.31) is a classical diffusion-advection-reaction (DAR) problem written in conservative form. With a suitable change of variables we are able to treat these PDE's equations likewise the linearized Non Linear Poisson equation in the previous section. Consider the Slotboom variable (2.32), we can rewrite system (3.31)

$$\begin{cases} \nabla \cdot \left(-qD_n e^{(\varphi^i/V_{th})} \nabla u_n \right) + \sigma_n^{i-1} e^{(\varphi^i/V_{th})} u_n & = & f^{i-1} & in\ \Omega_{Si} \\ u_n & = & n_D e^{(-\varphi^i/V_{th})} & on\ \Gamma_{D,Si} \\ \nabla u_n \cdot \mathbf{n} & = & 0 & on\ \Gamma_{N,Si} \end{cases}$$
$$(4.6)$$

We can easily obtain the weak formulation repeating the same steps made for the linearized Non Linear Poisson problem. Therefore the weak formulation of the Electron Continuity equation is: find $u_n \in H^1_{\Gamma_{D,Si}}(\Omega)$ such that:

$$\int_{\Omega_{Si}} qD_n e^{(\varphi^i/V_{th})} \nabla u_n \nabla v \, d\Omega + \int_{\Omega_{Si}} \sigma_n^{i-1} e^{(\varphi^i/V_{th})} u_n v \, d\Omega = \int_{\Omega_{Si}} f^{i-1} v \, d\Omega \qquad \forall v \in H^1_{\Gamma_{D,Si}}$$
$$(4.7)$$

The existence and uniqueness of the unkown variable u_n enures the same properties on n, thanks to the univocal relation between u_n and n. We have to make some hypotesis on the coefficients $\forall i \geq 0$:

- $qD_n e^{(\varphi^i/V_{th})} \in L^\infty(\Omega_{Si})$ and $\exists m$ s.t. $0 < m \leq qD_n e^{(\varphi^i/V_{th})}$ (a.e.) in Ω_{Si};

- $\sigma_n^{i-1} e^{(\varphi^i/V_{th})} \in L^\infty(\Omega_{Si})$ and $\exists m$ s.t. $0 < m \leq \sigma_n^{i-1} e^{(\varphi^i/V_{th})}$ (a.e.) in Ω_{Si}.

As we made before, we define the relative bilinear form

$$a(u,v) = \int_{\Omega_{Si}} qD_n e^{(\varphi^i/V_{th})} \nabla u_n \nabla v \, d\Omega + \int_{\Omega_{Si}} \sigma_n^{i-1} e^{(\varphi^i/V_{th})} u_n v \, d\Omega \qquad (4.8)$$

and the linear and bounded functional

$$F(v) = \int_{\Omega_{Si}} f^{i-1} v \, d\Omega \tag{4.9}$$

Now the well-posedness of this problem is ensured repeating the same passages showed in the previous section.

4.3 Numerical approximation

In this section we shall introduce briefly the classical Galerkin's method for the approximation of a weak formulation on Ω. Every weak formulation could be represented in a more compact and generic form as, find $u \in V$ such that

$$a(u, v) = F(v) \qquad \forall v \in V \tag{4.10}$$

where V is the space of admissible functions, e.g. $H^1_{\Gamma_D}(\Omega)$, $H^1_{\Gamma_{D,Si}}(\Omega_{Si})$. Let us introduce V_h which it is a family of finite-dimensional subspace of V, depending by a positive parameter h, such that

$$V_h \subset V, \quad dim V_h < \infty \, \forall h > 0 \tag{4.11}$$

The *Galerkin's problem* reads as, find $u_h \in V_h$ such that:

$$a(u_h, v_h) = F(v_h) \ \forall v_h \in V_h \tag{4.12}$$

Let be $\mathcal{T}_h$, a finite partition of Ω, and K a generic element of $\mathcal{T}_h$ such that $\bar{\Omega} = \bigcup \bar{K}$. In this case the parameter h refers to the characteristic dimension of the elements K. Let us introduce the general finite element spaces of the polynomial element-wise defined functions:

$$X^r_h(\Omega) := \{v_h \in C^0(\bar{\Omega}) : v_h|_K \in \mathbb{P}_r, \forall K \in \mathcal{T}_h\} \tag{4.13}$$

and the relative space where functions vanish on boundaries

$$X^r_{h,\Gamma_D}(\Omega) := \{v_h \in X^r_h : v_h|_{\Gamma_D} = 0\}. \tag{4.14}$$

If $\Omega \in \mathbb{R}^3$ we have:

$$dim \mathbb{P}_r := \frac{(r+1)^3}{2} + \frac{(r+1)^2}{2} + \frac{r(r+1)(2r+1)}{12} - \frac{r(r+1)^2}{2} - \frac{r(r+1)}{4} \tag{4.15}$$

More precisely we approximate $H^1_{\Gamma_D}(\Omega)$ with $X^1_{h,\Gamma_D}(\Omega)$ and $H^1_{\Gamma_{D,Si}}(\Omega_{Si})$ with $X^1_{h,\Gamma_{D,Si}}(\Omega_{Si})$. Therefore accordingly with (4.15) we have

$$dim\mathbb{P}_1 = 4$$
$$dimX_h^1 = N_h$$
$$dimX_{h,\Gamma_D}^1 = N_h - N_g$$

where N_h is the number of verteces of the partition $\mathcal{T}_h$ and N_g are the number of verteces lie on Dirichlet boundaries.

We denote by $\{\psi_j\}_{j=1}^{N_h}$ the Lagrangian basis of the space X_h^1. Naturally as $u_h \in X_h^1$ there are $u_j \in \mathbb{R}$ with $j = 1, ..., N_h$ such that:

$$u_h = \sum_{j=1}^{N_h} u_j \psi_j \tag{4.16}$$

Because every functions of V_h is a linear combination of ψ_i, we can test equation (4.12) only for each basis function rather than $\forall v_h \in V_h$. The result of the complete discretization is find u_j, with $j = 1, \ldots, N_h$ such that:

$$\sum_{j=1}^{N_h} u_j a(\psi_j, \psi_i) = F(\psi_i) \qquad \forall i = 1, \ldots, N_h \tag{4.17}$$

In order to implement this routine it's useful make explicit the subdivsion of the bilinear form on the element of the partition $\mathcal{T}_h$:

$$\sum_{j=1}^{N_h} u_j \sum_{K \in \mathcal{T}_h} a_K(\psi_j, \psi_i) = \sum_{K \in \mathcal{T}_h} F_K(\psi_i) \qquad \forall i = 1, \ldots, N_h \tag{4.18}$$

4.3.1 Geometrical discretization

We set every elements $K \in \mathcal{T}_h$ as a tetrahedral of volume $|K|$; we suppose that there exists a constant $\delta > 0$ such that:

$$\frac{h_K}{\rho_K} \leq \delta \qquad \forall K \in \mathcal{T}_h \tag{4.19}$$

where $h_k = diam(K) = max_{x,y \in K}|x - y|$ and ρ_K is the diameter of the sphere inscribed in the tetrahedral K. Condition (4.19) is the so called *mesh regularity condition* [Qua08] and it ensures an istropic partition. We denote with $\mathcal{E}_h$, $\mathcal{V}_h$ and $\mathcal{F}_h$ the set of all the edges, verteces and faces of $\mathcal{T}_h$ respectively, and for each $K \in \mathcal{T}_h$ we denote by ∂K and $\mathbf{n}_{\partial K}$ the boundary of the element and its outward unit normal.

4.3.2   Linearized Non Linear Poisson equation

As regards the linearized NLP equation we have:

$$a(\psi_j, \psi_i) = \int_\Omega \epsilon \nabla \psi_j \nabla \psi_i \, d\Omega + \int_\Omega \sigma^k \psi_j \psi_i \, d\Omega \qquad (4.20)$$

and the relative restriction on the element is

$$a_K(\psi_j, \psi_i) = \int_K \epsilon \nabla \psi_j \nabla \psi_i \, dK + \int_K \sigma^k \psi_j \psi_i \, dK \qquad (4.21)$$

Equation (4.21) it's formed by two distinct contributions, the former indentifies the diffusive contribution and generates the so called *stifness matrix*, while the latter refers to the reaction and generates the *mass matrix*.

The coefficient ϵ is a piece-wise costant function, which changes on different material regions. $\mathcal{T}_h$ is built such that every K belongs to a single region, while it is possible that verteces belong to different regions. Therefore ϵ is costant over each elements and integral in (4.21) become easier.

As a consequence of choose the discrete space X_h^1, we can't expect a better priori estimation error on the solution, than the first order respect the characteristic discretization step h_K referenza. This implies that is not necessary and useful the use of an high order quadrature, and the trapezoidal rule is enough accurate. The main consequence of using trapezoidal quadrature rule is that extra-diagonal elements of the mass-matrix disappear. This technique is well known as *lumping procedure* applied on the mass-matrix referenza.

Finally we obtain the contributions of the local system matrix A_K^k:

$$[A_K^k]_{ij} = \epsilon_K L_{ij} + \frac{|K|}{4}\sigma_i^k \qquad (4.22)$$

having set

$$\begin{aligned} L_{ij} &\simeq \int_K \nabla \psi_i \nabla \psi_j \, d\Omega \\[2mm] \sigma_i^k &= \sigma^k(\mathbf{x}_i) \end{aligned} \qquad (4.23)$$

Here follows the construction of the right hand side, based on the local contribution approximated with trapezoidal rule:

$$[F_K]_i^k = f_i^k |K|/4 \simeq \int_\Omega f^k \psi_i \, d\Omega \qquad (4.24)$$

The local contributions of each element K can be assembled in the global matrix A: let I be the global index of a generic vertex belonging to the

partition $\mathcal{T}_h$, we denote by $\mathcal{J}_K : \mathcal{V}_{\mathcal{T}_h} \to \mathcal{V}_K$ the map which connects I to its corresponding local index $i = 1, \ldots, 4$ in the element K. Then we have

$$A_{IJ}^k = \sum_{\substack{\forall K \in \mathcal{T}_h \, s.t. \\ \mathcal{J}_K(I), \mathcal{J}_K(J) \subset \mathcal{V}_K}} [A_K]_{ij}^k \qquad (4.25)$$

analogously for the force term $\mathbf{b}^{(k)}$:

$$b_I^k = \sum_{\substack{\forall K \in \mathcal{T}_h \, s.t. \\ \mathcal{J}_K(I) \subset \mathcal{V}_K}} [F_K]_i^k \qquad (4.26)$$

Once we have built the global matrix A^k and the global vector $\mathbf{b}^k$ we need to take into account the essential boundary conditions. In fact the displacement formulation is a primal formulation which forces Dirichlet boundary condition in a strong way. Therefore we have to modify the algebraic system. We choose the *diagonalization* techinique which does not alter the matrix pattern nor introduce ill-conditioning for the system. Let i_D be the generic index of a Dirichlet node, we denote by $[\delta\varphi_D]_i$ (which in this case is equal to zero) the known value of the solution $\delta\varphi$ at the node. We consider the Dirichlet condition as an equation of the form $a[\delta\varphi]_i = a[\delta\varphi_D]_i$, where $a \neq 0$ is a suitable coefficient. In order to avoid degrading of the global matrix condition number, we take a equal to the diagonal element of the matrix at the row i_D.

Finally we have completed the discretization of (Step 1), which reads as follows:

$$\begin{cases} A^k \delta\varphi^k & = & \mathbf{b}^k \\ \varphi^{k+1} & = & \varphi^k + \delta\varphi^k \end{cases} \qquad (4.27)$$

As every iteration procedure, problem (4.27) needs a suitable convergence break criterion. A good method is based on cheking the satisfaction of the fixed point equation (3.10) by the k-th solution, then the inner loop of the Gummel Map reads as: given a tollerance $toll > 0$ solve problem (4.27) untill:

$$||\mathbf{b}(\varphi^{k+1})||_2 > toll \qquad (4.28)$$

where $|| \cdot ||_2$ is the usual Euclideian norm for a vector.

Damping

Nevertheless the theorem (3.1), the system (4.27) may be affected by difficulties on the convergence velocity. The main problem associated with the

classical Newton method is the tendency to overestimate the length of the present correction step. This phenomenon is frequently termed as *overshoot*. In the case of the semiconductor equations this overshoot problem has often been treated by simply limiting the size of the correction vector $(\delta\varphi)$ determined by Newton's method. The usual established modifications to avoid overshoot are given by the follow formulations:

$$\tilde{A}(\varphi_k) = \frac{1}{t_k} A(\varphi_k) \tag{4.29}$$

t_k is a properly chosen positive parameter: for $t_k = 1$ the modified Newton methods reduce to the classical Newton method. We have now to deal with the question how to choose t_k or s_k such that the modified Newton methods exhibit superior convergence properties compared to the classical Newton method. For the case (4.29) there's a simple criterion suggested by Deuflhard [Sie84] t_k is taken from the interval $(0, 1]$ in such a manner that for any norm,

$$||A(\varphi_k)^{-1}\mathbf{b}(\varphi_k - t_k A(\varphi_k)^{-1}\mathbf{b}(\varphi_k))|| < ||A(\varphi_k)^{-1}\mathbf{b}(\varphi_k)|| \tag{4.30}$$

Condition (4.30) guarantees that the correction of the k-th iterate is an improved approximation to the final solution, in other words the residual norm can only descents. This condition can be easily evaluated only if the Jacobian matrix is factored into triangular matrices because the evaluation of the argument of the norm on the left hand side of (4.30) is then reduced to a forward and backward substitution and the evaluation of $\mathbf{b}(\varphi)$. Although we use an iterative methods (BCG solver) which implies serious diffuclties to the application of the above criterion. Another valid possibility is to use the main diagonal of $A(\varphi_k)$, denoted as $D(\varphi_k)$:

$$||D(\varphi_k)^{-1}\mathbf{b}(\varphi_k - t_k D(\varphi_k)^{-1}\mathbf{b}(\varphi_k))|| < ||D(\varphi_k)^{-1}\mathbf{b}(\varphi_k)|| \tag{4.31}$$

This is the criterion developed in our code. However the value to use for t_k is a question of trial and error. Frequently one chooses the following sequences:

$$t_k = \frac{1}{2^i} \tag{4.32}$$

$$t_k = \frac{1}{\frac{i(i+1)}{2}} \tag{4.33}$$

obiuvsly i is the subiterations of damping reached when satisfied (4.31). Sufficiently close to the solution (4.30) (and so (4.31)) will be satisfied with $t_k = 1$ so that the convergence properties of the classical Newton method are recovered.

4.3.3 Continuity equations

Let us write the discretized electron continuity equation in a suitable generic form on the K-th element:

$$\begin{cases} a_h^K(n_h, v_h) & = & \int_K J_h^K(n_h)\nabla v_h \, dK + \int_K \sigma n_h v_h \, dK \\[2mm] F(v_h)^K & = & \int_K f v_h \, dK \\[2mm] J_h^K & = & D_K(\bar{D}_n)\nabla(e^{(-\varphi/V_{th})}n_h) \end{cases} \quad (4.34)$$

Notice that we came back on carrier density variable, because finire spiegazione sulla difficolta numerica variabili di slotboom

We want to extend now the discussion about the treatment of the diffusive coefficient. The matrix $D_K(\bar{D}_n) \in \mathbb{R}^3$ can be characerized in three different ways:

$$D_K(\bar{D}_n) = \begin{cases} \mathcal{M}_K(\bar{D}_n)\,\mathcal{I} \\[2mm] \mathcal{H}_K(\bar{D}_n)\,\mathcal{I} \\[2mm] \dfrac{1}{|K|}\sum_{i=1}^{6}\mathcal{H}_{e_i}(\bar{D}_n)|e_i|s_i\mathbf{t}_i\mathbf{t}_i^T \end{cases} \quad (4.35)$$

These different approaches in the computation of the average of the diffusion coefficient are responsible for the quite different numerical perfomance of the relative methods. We already presented the standard average and the armonic average and we discussed briefly the advantages of them. Now we are interested in the latter method which is an exponentially fitted treatment of $\bar{D}_n$ over the entire subdomain K. From (4.34) we immeditaly obtain:

$$\mathbf{J}_h^K = \frac{1}{|K|}\sum_{i=1}^{6}|e_i|s_i j_{e_i}\mathbf{t}_i \quad (4.36)$$

Having defined the flux vector over K in the form (4.36), it is clearly possible to construct a fimily of Galerkin finite element approximations for the continuity equations by a proper choice of the quantities j_{e_i}.

Edge flux density computation

We introduce an approximate flux density computation along the edges of ∂K based on the classical one dimensional *Sharfetter-Gummel* method referenza o anticipazione?. For each edge e_i, the tangential component of $J_h^K(n_h)$ is defined as:

$$j_{e_i} \simeq \mathcal{H}_{e_i}(\bar{D}_n) \frac{\mathcal{B}(\delta_i(\varphi/V_{th}))n_{h,k} - \mathcal{B}(-\delta_i(\varphi/V_{th}))n_{h,j}}{|e_i|} \tag{4.37}$$

where

$$\delta_i(\varphi/V_{th}) = \frac{\varphi_k - \varphi_j}{V_{th}} = 2\frac{(\mathbf{b}_K \cdot \mathbf{t}_{e_i})|e_i|}{2\mathcal{H}_{e_i}(\bar{D}_n)} = 2\gamma_i \tag{4.38}$$

$$\mathcal{B}(z) = \begin{cases} \dfrac{z}{e^z - 1} & z \neq 0 \\ 1 & z = 0 \end{cases} \tag{4.39}$$

being $\mathbf{b}_K$ the relative drift component of the problem on K and $|\gamma_i|$ the Pèclet number associated with the edge e_i.

The discretization scheme

The local contributions to the assembling of the global stiffness matrix and load vector associated with the linear algebraic system read as follows:

$$\Phi_K = \begin{bmatrix} -\begin{pmatrix} a_{e12}\mathcal{B}_{12}L_{21}^K + \\ a_{e13}\mathcal{B}_{13}L_{31}^K + \\ a_{e14}\mathcal{B}_{14}L_{41}^K \end{pmatrix} & a_{e12}\mathcal{B}_{12}L_{21}^K & a_{e13}\mathcal{B}_{13}L_{31}^K & a_{e14}\mathcal{B}_{14}L_{41}^K \\ a_{e21}\mathcal{B}_{21}L_{12}^K & -\begin{pmatrix} a_{e21}\mathcal{B}_{21}L_{12}^K + \\ a_{e23}\mathcal{B}_{23}L_{32}^K + \\ a_{e24}\mathcal{B}_{24}L_{42}^K \end{pmatrix} & a_{e23}\mathcal{B}_{12}L_{32}^K & a_{e24}\mathcal{B}_{12}L_{42}^K \\ a_{e31}\mathcal{B}_{31}L_{31}^K & a_{e31}\mathcal{B}_{32}L_{32}^K & -\begin{pmatrix} a_{e31}\mathcal{B}_{31}L_{31}^K + \\ a_{e32}\mathcal{B}_{32}L_{32}^K + \\ a_{e34}\mathcal{B}_{34}L_{34}^K \end{pmatrix} & a_{e34}\mathcal{B}_{34}L_{34}^K \\ a_{e41}\mathcal{B}_{41}L_{41}^K & a_{e42}\mathcal{B}_{42}L_{42}^K & a_{e43}\mathcal{B}_{43}L_{43}^K & -\begin{pmatrix} a_{e41}\mathcal{B}_{41}L_{41}^K + \\ a_{e42}\mathcal{B}_{42}L_{42}^K + \\ a_{e43}\mathcal{B}_{43}L_{43}^K \end{pmatrix} \end{bmatrix} \tag{4.40}$$

$$A_K = \Phi_K + \frac{|K|}{4}diag(\sigma_n) \tag{4.41}$$

$$\mathbf{F}_K = \frac{|K|}{4}(f_1, f_2, f_3, f_4)^T \tag{4.42}$$

Vale la seguente uguaglianza?

$$L_{ij} = s_{ij}\mathbf{t}_{ij} \cdot \nabla\psi_i \tag{4.43}$$

Capitolo 5

Simulation results

5.1 Case tests presentation

In this section we dedicate some words to give informations about what kind of input file FEMOS get in input and what files it produces. Basically all .tdr format are accepted by FEMOS code. For our simulation it was possible used synopsis tools. More precisely the device design was performed with SDE and the mesh generator used was SNMESH. About output we produce .xmf files easly visible with paraview.

We focus our tests over three main structures: diode, diode inside an oxide box and a transistor mos. Here we presents the geometry tested and some mesh pattern used.

(a) (b) (c)
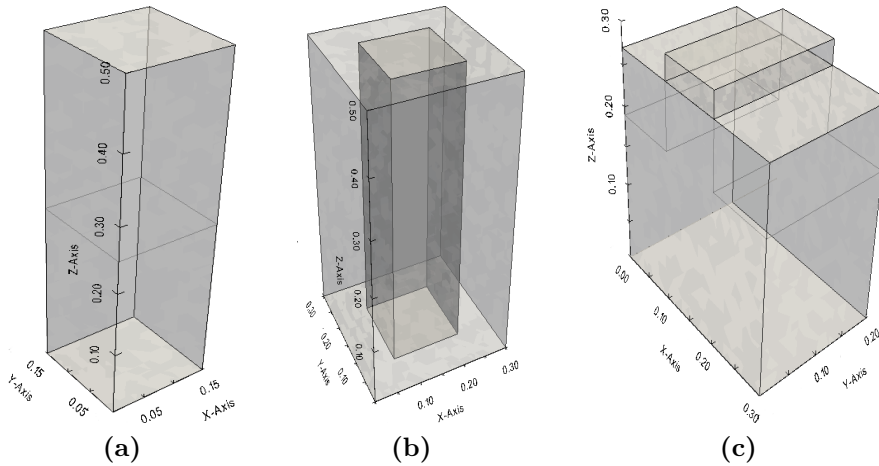
For everyone of these case test we investigated different doping concentration and distribution (like abrupt or gauss profile), multiple generation/-

recombination and mobility models applyed, ... Results are always checked
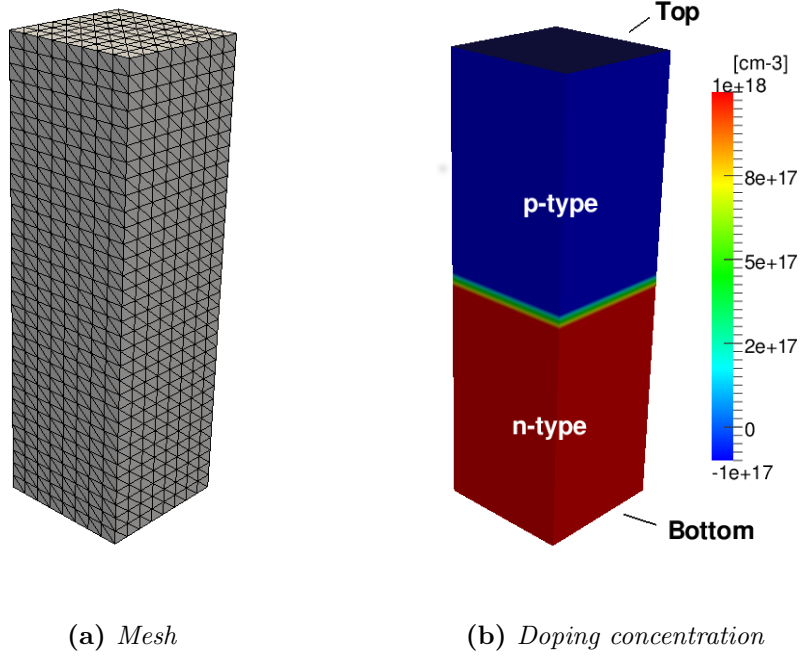with the SDEVICE simulation ...

(a) *Mesh* (b) *Doping concentration*

Figura 5.1: Geometry of case test Diode.
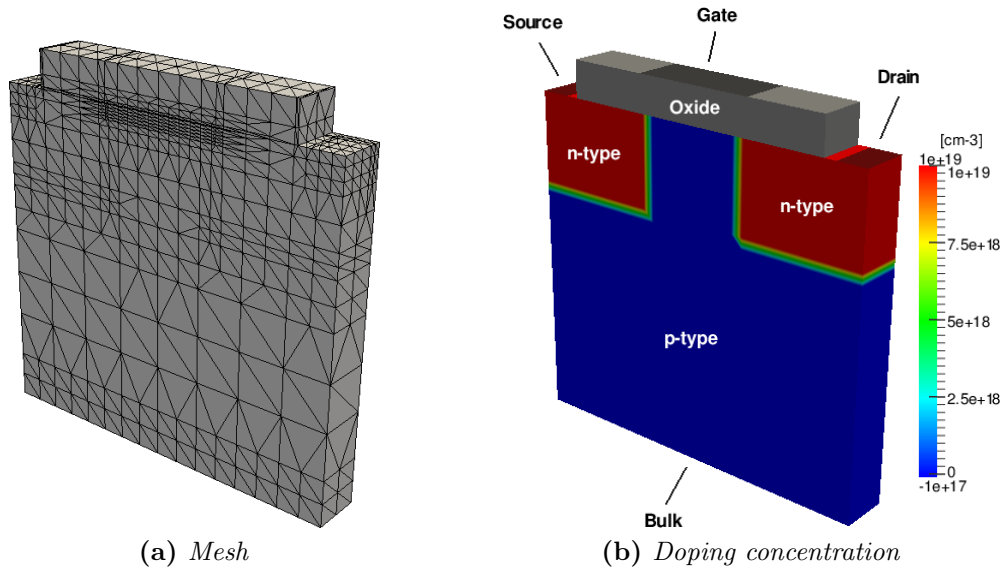

(a) *Mesh* (b) *Doping concentration*

Figura 5.2: Geometry of case test MOS n-channel.

Capitolo 6

The current calculation problem

In many physical and engineering problems the real interesting variable of the conservation law is the flux in the domain or on specific surfaces and boundaries. The study of micro and nano electronics devices doesn't except this observation, in fact most of all models are oriented to obtain a satisfactory description of the current density. We know that the primal and not mixed formulation for the continuity equation doesn't resolved the flux density. The conseguence of this fact is a binding post-processing of the quantities computed in order to reconstruct the current density of electrons and holes. It's evident which this part covers a lead role in the device simulation: as we are satisfied of the impressive results of the finite element scheme, it will be reather regrettable to lost the accuracy of our simulation during the computation of the current density. About this question many academics propose different solutions and the relative literature is boundless. Nevertheless the problem shows various aspects to take into account, among these there are some which every good method should be respect:

- reduced computational cost;

- easy extension to 3D simulation;

- detains some useful properties like orthogonal conservation across a generic surface of the domain;

- preserve consistency with the numerical scheme adopted.

It's not trivial ensure everyone of these points, thus move on toward a unique choice of a method is a delicate matter. Luckily there's some *main stone* which offers ever a good start point whence achieve new results. Probably

the most known and recognized by the inherent literature is the *Sharfetter-Gummel formula.*
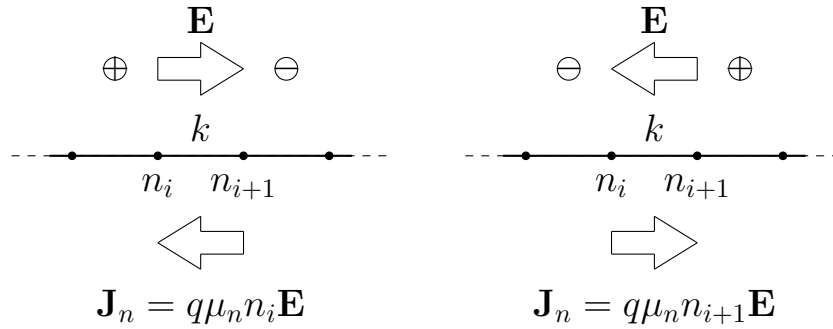
6.1   Scharfetter-Gummel formula

Consider the resolution of the continuity equation along a monodimensional domain. For the sake of simiplicity we contemplate a uniform partition (this hypotesis is not necessary for a more generic analysis). Moreover on every nodes is defined the electrostatic potential φ, and on every elements the relative electrostatic field $\mathbf{E}$. In order to avoid redundant considerations and calculuses, we proceed with our analysis considering only the current density of electrons ($\mathbf{J}_n$).

In 1969 D. Scharfetter and H.K. Gummel (two scientists of Bell Labs), introduced a formula to compute the current density in this case, given φ and the density solution (n) on every nodes. This innovative approach led for the twenty years to follow every simulation which contemplates electric-devices.

We know that the constituve law is composed by a drift component, which depends on the electric field, and a diffusion component, which depends on the variation of the carrier density. Consider a generic element K, we define the drop in voltage $\Delta\varphi^k = \varphi_{i+1} - \varphi_i$. There are three possible situations which are well explain in the picture:

- $\Delta\varphi \gg 0$, mainly drift component from right to left

- $\Delta\varphi \ll 0$, mainly drift component from left to right

- $\Delta\varphi \simeq 0$, mainly diffusion component

With the $Sharfetter - Gummel$ formula it's possibile taking into account every of these situations and solve boundary layer problems which occurs often in presence of strong drift component contribute.

$$J_n^k = q\frac{D_n}{h}\left[n_{i+1}\mathcal{B}\left(\frac{\Delta\varphi^k}{V_{th}}\right) - n_i\mathcal{B}\left(-\frac{\Delta\varphi^k}{V_{th}}\right)\right] \tag{6.1}$$

In the latter case $\Delta\varphi = 0$) the formula became:

$$J_n^k = qD_n\frac{n_{i+1} - n_i}{h} \tag{6.2}$$

which is the correct approximation of the current density using $\mathbb{P}_1$ basis.

Morover many mathematics discover important properties about this method questa parte la vorrei fare meglio. These changes in the direction of the electric field lead to boundary layer problems. It's not possibile afford these situations with a simply upwinding sheme ...

6.2 Extension for the 3D case

The extension of this formula for the 3D case is not trivial. We show the method for the computation of the current density of electrons (the extension for the current density of holes is quite similar). We remark the quasi fermi formula for current density:

$$\mathbf{J}_n = -q\mu_n n\nabla\varphi_n \tag{6.3}$$

where φ_n is the quasi fermi potential level. Let us write (5.3) in function of potential and in a canonic form:

$$\mathbf{J}_n\frac{exp\left(\dfrac{\varphi_n - \varphi}{V_{th}}\right)}{q\mu_n n_i} + \nabla\varphi_n = 0 \tag{6.4}$$

We consider $\mathbf{J}_n \in [L^2(\Omega)]^3$ and $\varphi_n, \varphi \in H^1(\Omega)$. We are able to multiply (5.4) with a generic function $\mathbf{q} \in [L^2(\Omega)]^3$ and then intagrate over the domain Ω:

$$\int_\Omega \frac{exp\left(\dfrac{\varphi_n - \varphi}{V_{th}}\right)}{q\mu_n n_i}\mathbf{J}_n \cdot \mathbf{q}\,d\Omega + \int_\Omega \nabla\varphi_n \cdot \mathbf{q}\,d\Omega = 0 \tag{6.5}$$

We proceed taking the usual discrete space of the constant elemenwise functions:

$$V_h = \left\{w \in L^2(\Omega) : w|_K \in \mathbb{P}_0 \forall K \in \tau_h\right\} \tag{6.6}$$

Now the discrete quantities are $\mathbf{J}_n^h \in [V_h]^3$ and $\nabla\varphi_n^h \in V_h$. We desire produce a system of equation on every elements for the three componente of $\mathbf{J}_n$, this is possible with a smart choice of the test function $\mathbf{q}_h \in [V_h]^3$:

$$\mathbf{q}_{1,2,3}^h = \left\{ \begin{bmatrix} 1 \\ 0 \\ 0 \end{bmatrix} \begin{bmatrix} 0 \\ 1 \\ 0 \end{bmatrix} \begin{bmatrix} 0 \\ 0 \\ 1 \end{bmatrix} \right\} \tag{6.7}$$

From (5.5) we obtain the sequent system of equations defined for every element of the mesh:

$$\int_K \frac{exp\left(\dfrac{\varphi_n - \varphi}{V_{th}}\right)}{q\mu_n n_i} \mathbf{J}_n^h \cdot \mathbf{q}_i^h \, dK + \int_K \nabla\varphi_n^h \cdot \mathbf{q}_i^h \, dK = 0 \qquad \forall i = 1, 2, 3 \tag{6.8}$$

Operating the intagration we obtain the sequent formula for the current density components:

$$[\mathbf{J_n}]_i = -\mathbb{H}_K\left(q\mu_n n_i exp\left(\frac{\varphi - \varphi_n}{V_{th}}\right)\right) \frac{\partial\varphi_n^h}{\partial x_i} \quad i = 1...d \quad \forall K \in \tau_h \tag{6.9}$$

where $\mathbb{H}_K(f)$ is the armonic average on the elment K of the function f.

Although resolve the armonic average with a comlete 3D integration may be expensive in calculation time and propably not necessary. One approximation of this integral would be pass from a 3D integration to 1D integration along one edge of the element K.

$$\left(\frac{\int_K f^{-1} \, dK}{|K|}\right)^{-1} \simeq \left(\frac{\int_{e*} f^{-1} \, de}{|e^*|}\right)^{-1} \tag{6.10}$$

The approximation (5.10) is valid if we consider the correct edge.

Consider a quantity defined on the verteces:

$$\Phi := \varphi - \varphi_n \tag{6.11}$$

which is the difference between the electrostatic potential and the quasi fermi potential level. Now for every element consider two vertices: $\mathbf{x}_m$ s.t. $\Phi(\mathbf{x}_m) = \Phi_m := min_K(\Phi)$ and $\mathbf{x}_M$ s.t. $\Phi(\mathbf{x}_M) = \Phi_M := max_K(\Phi)$. Obviously it exists only one edge which connects these two points and on this one we perform the 1D integration (5.10). First of all as we reduce the dimension is feasible to represent $\sigma(\mathbf{x})$ in a easier mode as follows:

$$\sigma_n(s) = q\mu_n n_i exp\left(\Phi_m + (\Phi_M - \Phi_m)\frac{s - s_m}{|e^*|}\right) \tag{6.12}$$

where $s \in [s_m, s_M]$ is the parameter refered to the edge e^* s.t. $\sigma_n(s_m) = \sigma_n(\mathbf{x}_m)$ and $\sigma_n(s_M) = \sigma_n(\mathbf{x}_M)$. We can easily resolve (5.10) with the substitution of variable:

$$\eta := \frac{s - s_m}{|e^*|}$$

this lead us to the sequent steps of integration:

$$
\begin{aligned}
\int_{e^*} \sigma_n^{-1}\, de &= |e^*| \int_0^1 \frac{exp\left(-\Phi_m - (\Phi_M - \Phi_m)\eta\right)}{q\mu_n n_i}\, d\eta \\
&= |e^*| \frac{exp(-\Phi_m)}{q\mu_n n_i} \frac{exp(\Phi_m - \Phi_M) - 1}{\Phi_m - \Phi_M} \\
&= |e^*| \frac{exp(-\Phi_m)}{q\mu_n n_i} \frac{1}{\mathbf{B}(\Phi_m - \Phi_M)}
\end{aligned}
$$

finally we obtain:

$$\int_K \sigma_n^{-1}\, dK \simeq q\mu_n n_i exp(\Phi_m)\mathbf{B}(\Phi_m - \Phi_M) \tag{6.13}$$

Similar results may be obtained repeating the integration and considering s_M as start point:

$$\int_K \sigma_n^{-1}\, dK \simeq q\mu_n n_i exp(\Phi_M)\mathbf{B}(\Phi_M - \Phi_m) \tag{6.14}$$

Numerical results (qua sarebbe carino fare un po' di test con una parte o l'altra della formula per mettere in crisi) shows that the best choice is e linea combination of these approzimations as follows:

$$\mathbf{J_n}^K = -q\mu_n \left[\frac{n_{min}\mathbf{B}(-\Delta\Phi_{max}) + n_{max}\mathbf{B}(\Delta\Phi_{max})}{2}\right]\nabla\varphi_n^h \tag{6.15}$$

This approach is the natrual extension of the *Sharfetter − Gummel* formula for the 1D case, indeed it's possible demonstrate the equivalence assuming a monodimensionale domain.

6.3 Residue Method

Contact method

In the following we present an accurate method for the evaluation of boundary integrals in semiconductor device based on the work . It's well known that the evaluation of boundary integrals is a difficult task occuring routinely in electron device simulations. In general, given a contact Γ_i, fluxes of current density to be calculated assume the following form:

$$\mathcal{I}_i^\nu = \int_{\Gamma_i} \mathbf{J}_\nu(\nu) \cdot \mathbf{n} \, d\Gamma_i \qquad \nu = \{n, p\} \tag{6.16}$$

where as usual $\mathbf{n}$ is the unit outward normal of the domain boundary. Difficulties in the numerical evalutaion of (5.16) arise from singularities in spatial derivatives of the approximate solution n^h or p^h near the contact edges, due to a change in the boundary condition type (from Dirichlet to Neumann) at the contact ends. In this work we extend the residue method on the 3D case and we confirm the optimal results obtained previously, matching them with SDEVICE (come bisogna scirvere il software che politica usare?). Moreover we remark that the method can be succesfully applied to a wide spread of applications, including contact charges, carrier quantum probability fluxes and heat fluxes.

Before go further with the presentation of the results, it's useful look up the anlysis made in Citazione and adapt it to our case. Before applying boundary conditions, the discretized form of referenza equazione reads:

$$\sum_{j\in\eta} A_{ij}\nu_j\psi_j(x_j) = b_i \qquad \forall i \in \eta \tag{6.17}$$

in FEMOS simulations A_{ij} is the K_{FVSG} global matrix but it's possibile use every discretization scheme. We can split the set of total nodes in contact node η_g and the complementary part η_n. The values of ν_j are known on the contacts and (5.17) can be rewritten as follows:

$$\begin{cases} \sum_{j\in\eta_n} A_{ij}\nu_j\psi_j(x_j) = b_i - \sum_{j\in\eta_g} A_{ij}\nu_j\psi_j(x_j) & \forall i \in \eta_n \\[2ex] \sum_{j\in\eta_n} A_{ij}\nu_j\psi_j(x_j) = b_i - \sum_{j\in\eta_g} A_{ij}\nu_j\psi_j(x_j) & \forall i \in \eta_g \end{cases} \tag{6.18}$$

The first set of equations is then solved for the problem unknowns ν_j (carrier density) while the second can be used for boundary flux estimation
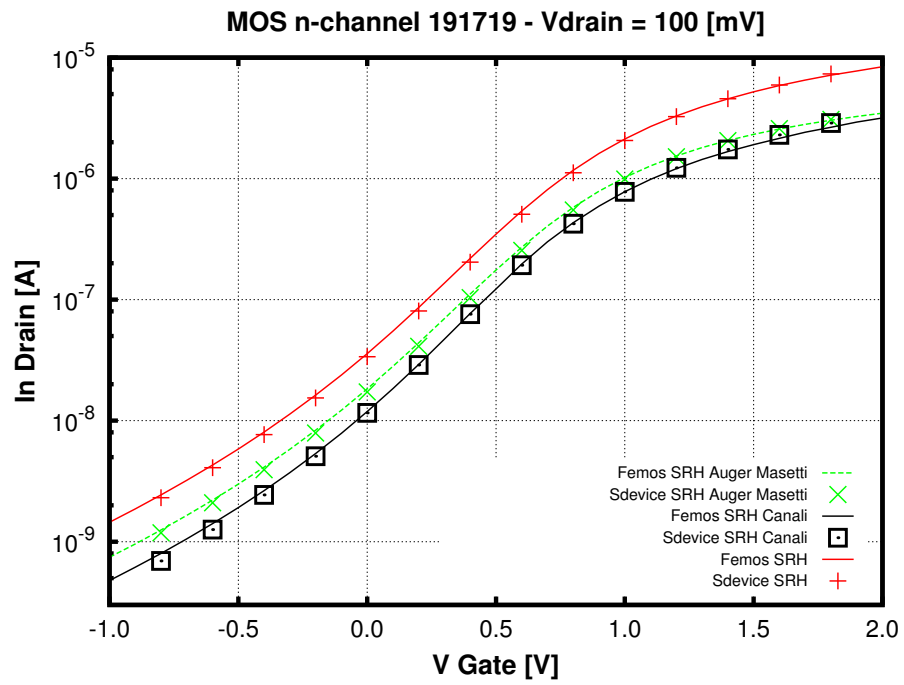
as described in the folowing. Consider a different test function v_i^h defined as:

$$v_i^h = \sum_{j \in \eta_{gi}} \psi_j \tag{6.19}$$

where η_{gi} is the set of nedes lying on contact Γ_i. We can rewrite (5.16) as follows:

$$
\begin{aligned}
\mathcal{I}_i^\nu &= \int_{\Gamma_i} \mathbf{J}_\nu(\nu) \cdot \mathbf{n} \, d\Gamma_i = \sum_{j=1}^{n_d} \int_{\Gamma_j} \mathbf{J}_\nu(\nu) \cdot \mathbf{n} \, v_i^h \, d\Gamma_j \\
&= \sum_{i \in \eta_{gi}} \sum_{j=1}^{n_d} \int_{\Gamma_j} \mathbf{J}_\nu(\nu) \cdot \mathbf{n} \, \psi_i \, d\Gamma_j = \sum_{i \in \eta_{gi}} \int_{\partial\Omega} \mathbf{J}_\nu(\nu) \cdot \mathbf{n} \, \psi_i \, d\partial\Omega \\
&= \sum_{i \in \eta_{gi}} \left[\int_\Omega \nabla \cdot \mathbf{J}_\nu(\nu) \psi_i \, d\Omega + \int_\Omega \mathbf{J}_\nu(\nu) \cdot \nabla \psi_i \, d\Omega \right] \\
&= \sum_{m \in \eta_{gi}} \left[\sum_{j \in \eta} A_{ij} \nu_j \psi_i - b_i \right]
\end{aligned}
\tag{6.20}
$$

Results

Bulk method

Now the question is: it's possible extend the residue technique at the calculation of current inside the domain? The answer at this question is not trivial. A good start point is the work of J.R. Hughes and Larson in the article The Continuous Galerikin Method Is Locally Conservative.The aim of their work is well exposed in the title and the conclusion is that this important property (locally conservation) is ensured less than the existence of an **auxiliary flux** denoted as $H(\omega)$ (with $\omega \subseteq \Omega$). To extract the statement of global and local conservation from the variational formulation, thay need to be able to set the weighting function to one. Obviously this is possible if $\Gamma_g = \varnothing$. In order to include every case an extended weak formulation is presented: consider η the set of all verteces of the discrete domain and η_g the subset of verteces on Dirichlet boundaries. Now we are able to define the discrete space $\mathcal{V}^h := span\{\psi_i\}_{i \in \eta - \eta_g}$ and $V^h := \mathcal{V}^h \oplus span\{\psi_i\}_{i \in \eta_g}$, where ψ_i is the basis function assiociated with the node i. The last space is the completion of the usual finite element space $(\mathcal{V}^h)$. Note that the constant function having value 1 is contained in V^h. The modified form of Galerkin's method is given by:

Find $u^h \in \mathcal{S}^h$ and $H^h(\Omega) \in V^h - \mathcal{V}^h$ such that

$$(W^h, H^h(\Omega))_{\Gamma_g} = B(W^h, u^h) - L(W^h) \qquad \forall W^h \in V^h \qquad (6.21)$$

Note that (5.21) splits into two subproblems:

$$0 = B(w^h, u^h) - L(w^h) \qquad \forall w^h \in \mathcal{V}^h \qquad (6.22)$$

$$(W^h, H^h(\Omega))_{\Gamma_g} = B(W^h, u^h) - L(W^h) \qquad \forall W^h \in V^h - \mathcal{V}^h \qquad (6.23)$$

Equation (5.23) is a problem which determines $H^h(\Omega)$. In it we assume u^h is already determined by (5.22). The coefficient matrix for (5.23) is the mass matrix associated with Γ_g

$$\sum_{j \in \eta_g} (\psi_i, \psi_j) H_j^h(\Omega) = B(\psi_i, u^h) - L(\psi_i) \qquad \forall i \in \eta_g \qquad (6.24)$$

Il prodotto sul bordo genera la medesima matrice di massa?E cosa succede nei punti che non sono di Dirichlet?Non pu essere formulato in questo modo il problema?

In ogni caso noi abbiamo provato ad estendere il secondo problema ad ogni elemento interno che intersechi o meno i bordi di Dirichlet. Questo a cosa corrsiponde?

Abbiamo interpretato la costruzione per elemento come se in ogni elemento il problema avesse delle condizioni di dirichlet che si affacciano con

gli altri elementi adiacenti. Se assumiamo che questa procedura sia corretta allora penso che i successivi ragionamenti stiano in piedi.

Sempre nell'articolo viene testata la formulazione estesa contro la funzione test costante e si ottiene la seguente equivalenza:

$$\int_{\Gamma_g} H^h(\Omega) \, d\Gamma = \int_{\Gamma_h^+} (a_n u^h - h^+) \, d\Gamma - \int_{\Gamma_h^-} h^- \, d\Gamma - \int_\Omega f \, d\Omega \qquad (6.25)$$

avendo assunto ogni nodo come Dirichlet allora valgono le seguenti affermazioni:

- $\Gamma_g = \partial\Omega$

- $\Gamma_h = \varnothing$

quindi possiamo affermare che per ogni elemento vale:

$$\int_{\partial\Omega} H^h(\Omega) \, d\Gamma = - \int_\Omega f \, d\Omega \qquad (6.26)$$

Ora vorrei ripartire dal problema di partenza:

$$
\begin{aligned}
-\nabla \cdot \mathbf{J} &= f \\
\int_\Omega -\nabla \cdot \mathbf{J} \Psi_k \, d\Omega &= \int_\Omega f \Psi_k \, d\Omega \qquad \forall k = 1...N_{elements} \\
\int_K -\nabla \cdot \mathbf{J} \, d\Omega &= \int_K f \, d\Omega \qquad \forall k = 1...N_{elements} \\
\int_{\partial K} -\mathbf{J} \cdot \mathbf{n} \, d\Omega &= \int_K f \, d\Omega \qquad \forall k = 1...N_{elements}
\end{aligned}
\qquad (6.27)
$$

La domanda quindi è possiamo in qualche modo dire che:

$$H^h(K) = \mathbf{J} \cdot \mathbf{n} \qquad (6.28)$$

Entrambe le quantità sono definite sul bordo dell'elemento, inoltre la ricostruzione dalle componenti normali al vettore densità di corrente non è impossibile. Tuttavia occorre passare prima a definire la grandezza sulle facce del tetraedro:

- Calcolo delle quantità nodali $H_j^h(\Omega)$

- Redistribuzione dei valori sulle facce (metodo percentuale proporzionalmente alle aree) $\bar{H}_j^h(\Omega)$

- Ortogonalizzazione dei contributi normali alle facce $\bar{H}_j^h(\Omega)\mathbf{n}_j$ tramite procedura alla Grand-Shmidt $H_j^*\mathbf{n}_j^*$

- Calcolo del vettore densità di corrente nell'elemento $\mathbf{J} = \sum_{i=1}^4 H_j^*\mathbf{n}_j^*$

6.4 The Residue Method

6.4.1 Idea

Nel calcolo della corrente ai contatti si calcola sostanzialmente il residuo del problema DD globale, utilizzando però la matrice di sistema non ancora modificata per le condizioni al bordo di Dirichlet. Infine dato un contatto (e quindi un insieme di vertici), si sommano le componenti del residuo relative ai vertici che risiedono su quel contatto. In questo modo otteniamo la corrente di elettroni $\mathcal{I}_n^k$ (k-esimo contatto). Possiamo affermare ovviamente che:

$$\mathcal{I}_n^k = \int_{\Gamma_k} \mathbf{J}_n \cdot \mathbf{n} \, d\Gamma_k \qquad (6.29)$$

Poniamo di aver risolto il problema e di conoscere le densità su ogni vertice della triangolazione.**L'idea principale è di pensare ad ogni singolo elemento come un nuovo problema con condizioni di Dirichlet sui quattro vertici.** Applico nuovamente l'idea del calcolo della corrente ai contatti utilizzata per l'intero dominio di simulazione, ma questa volta ogni faccia del tetraedro costituisce un contatto. Quindi calcolo la matrice locale e la forzante locale del problema ed infine computo il residuo con la soluzione che già possiedo. Ora non mi resta che per ogni faccia (contatto) calcolare la corrente.

Assumendo $\mathbf{J}_n$ nel discreto essa è una quantità definita sugli elementi, dunque sarà costante nel dominio che stiamo considerando in questo momento, possiamo affermare che data una faccia k dell'elemento:

$$\mathcal{I}_n^k = \mathbf{J}_n \cdot \mathbf{n}_k |\Gamma_k| \qquad (6.30)$$

Così facendo è possibile recuperare quattro contributi alla corrente dell'elemento che tramite un'ortogonalizzazione alla Grand-Schmidt ci permettono di ricostruire il vettore densità di corrente.

$$
\begin{aligned}
\mathbf{J}_n \;=\;& \mathcal{I}_n^1 \mathbf{n}_1 + (\mathcal{I}_n^2 \mathbf{n}_2 - \mathcal{I}_n^2 (\mathbf{n}_2 \cdot \mathbf{n}_1) \mathbf{n}_1) \\
&+ (\mathcal{I}_n^3 \mathbf{n}_3 - \mathcal{I}_n^3 (\mathbf{n}_3 \cdot \mathbf{v}_2) \mathbf{v}_2) + (\mathcal{I}_n^3 \mathbf{n}_3 - \mathcal{I}_n^3 (\mathbf{n}_3 \cdot \mathbf{n}_1) \mathbf{n}_1) \\
&+ (\mathcal{I}_n^4 \mathbf{n}_4 - \mathcal{I}_n^4 (\mathbf{n}_4 \cdot \mathbf{v}_3) \mathbf{v}_3) + (\mathcal{I}_n^4 \mathbf{n}_4 - \mathcal{I}_n^4 (\mathbf{n}_4 \cdot \mathbf{v}_2) \mathbf{v}_2) + (\mathcal{I}_n^4 \mathbf{n}_4 - \mathcal{I}_n^4 (\mathbf{n}_4 \cdot \mathbf{n}_1) \mathbf{n}_1)
\end{aligned}
$$

Mi sembra una possibile estensione del metodo dei residui all'interno del dispositivo anche se probabilmente potrei avere commesso degli errori nello sviluppo dell'idea. Tuttavia anche nel caso di una corretta base teorica, per come ho presentato il metodo mi sembra che si rischi di incorrere in problemi numerici date le numerosi differenze che occorrerebbe fare.

Probabilmente aiutandoci con gli articoli di Hughes possiamo tirar fuori un'idea simile, sfruttando in qualche modo i flussi ausiliari che sono senza dubbio legati ai residui dei problemi locali.

Bibliografia

[Qua08] Alfio Quarteroni. *Modellistica Numerica per Problemi Differenziali.* Springer Italia, Milan, 2008.

[Sal10] Sandro Salsa. *Equazioni a Derivate Parziali, metodi, modelli e applicazioni.* Springer Italia, Milan, 2010.

[Sie84] Selberherr Siegfried. *Analysis and Simulation of Semiconductor Devices.* Springer-Verlag, Wien, 1984.

[YT09] Taur Yuan and H. Ning Tak. *Fundamentals of Modern VLSI Devices.* Cambridge University Press, 2009.